The Plant Cell, Vol. 19: 3593–3609, November 2007, www.plantcell.org © 2007 American Society of Plant Biologists

Comparison of *Petunia inflata S*-Locus F-Box Protein (Pi SLF) with Pi SLF–Like Proteins Reveals Its Unique Function in S-RNase–Based Self-Incompatibility [W]

Zhihua Hua,[a] Xiaoying Meng,[a] and Teh-hui Kao[a,b,1]

[a] Intercollege Graduate Degree Program in Plant Biology, Pennsylvania State University, University Park, Pennsylvania 16802
[b] Department of Biochemistry and Molecular Biology, Pennsylvania State University, University Park, Pennsylvania 16802

Petunia inflata **possesses S-RNase–based self-incompatibility (SI), which prevents inbreeding and promotes outcrossing. Two polymorphic genes at the *S*-locus, *S-RNase* and *P. inflata S*-locus F-box (Pi *SLF*), determine the pistil and pollen specificity, respectively. To understand how the interactions between Pi SLF and S-RNase result in SI responses, we identified four Pi *SLF–like* (Pi *SLFL*) genes and used them, along with two previously identified Pi *SLFL*s, for comparative studies with Pi SLF_2. We examined the in vivo functions of three of these Pi SLFLs and found that none functions in SI. These three Pi SLFLs and two other Pi SLFs either failed to interact with S_3-RNase (a non-self S-RNase for all of them) or interacted much more weakly than did Pi SLF_2 in vitro. We divided Pi SLF_2 into FD1 (for Functional Domain1), FD2, and FD3, each containing one of the Pi SLF–specific regions, and used truncated Pi SLF_2, chimeric proteins between Pi SLF_2 and one of the Pi SLFLs that did not interact with S_3-RNase, and chimeric proteins between Pi SLF_1 and Pi SLF_2 to address the biochemical roles of these three domains. The results suggest that FD2, conserved among three allelic variants of Pi SLF, plays a major role in the strong interaction with S-RNase; additionally, FD1 and FD3 (each containing one of the two variable regions of Pi SLF) together negatively modulate this interaction, with a greater effect on interactions with self S-RNase than with non-self S-RNases. A model for how an allelic product of Pi SLF determines the fate of its self and non-self S-RNases in the pollen tube is presented.**

INTRODUCTION

Flowering plants that produce bisexual flowers have a strong tendency to self-pollinate, due to the close proximity of the female (pistil) and male (anther) reproductive organs. As self-fertilization results in reduced fitness in the progeny and decreased genetic diversity in the species, many flowering plants have adopted strategies to prevent self-pollination and promote outcrossing. One such strategy is self-incompatibility (SI), which allows pistils to reject genetically related (self) pollen but to accept genetically unrelated (non-self) pollen for fertilization (de Nettancourt, 2001). SI in the Solanaceae, Rosaceae, and Plantaginaceae families employs S-RNase as the pistil specificity determinant (Lee et al., 1994; Murfett et al., 1994; Xue et al., 1996) and the *S*-locus F-box (abbreviated SLF or SFB) protein as the pollen specificity determinant (Lai et al., 2002; Entani et al., 2003; Ushijima et al., 2003; Qiao et al., 2004a, 2004b; Sijacic et al., 2004; Sonneveld et al., 2005; Tsukamoto et al., 2006). Both the *S-RNase* and *SLF* genes are located at the highly polymophic *S*-locus. If the *S*-haplotype of pollen matches one of the two *S*-haplotypes of the pistil, the pollen is recognized by the pistil as self pollen and the growth of its tube in the style is inhibited. Pollen that carries a different *S*-haplotype than those carried by the pistil is recognized as non-self pollen and is accepted for fertilization. S-RNases are secreted into the intercellular space of the transmitting tract of the pistil and are taken up by pollen tubes in a non-*S*-haplotype–specific manner, as shown by immunocytochemical experiments (Luu et al., 2000; Goldraij et al., 2006).

The observations that the RNase activity of S-RNases is essential for their function in the rejection of self pollen tubes (Huang et al., 1994) and that pollen rRNAs were degraded upon incompatible pollination but not compatible pollination (McClure et al., 1990) have led to the hypothesis that only self S-RNase is able to exert its cytotoxic action inside a pollen tube. Recent identification of SLF of *Petunia inflata* (Pi SLF) as the pollen specificity determinant (Sijacic et al., 2004) has allowed us to examine this hypothesis. Most of the F-box proteins whose functions have been characterized to date are components of a type of multisubunit E3 ubiquitin ligase complex, named SCF (for Skp1, Cullin, F-box), which is composed of Skp1, Cullin-1, F-box protein, and Rbx1 and which, along with E1 ubiquitin-activating enzyme and E2 ubiquitin-conjugating enzyme, is involved in ubiquitin-mediated protein degradation by the 26S proteasome (for reviews, see Cardozo and Pagano, 2004; Moon et al., 2004; Smalle and Vierstra, 2004). We have previously shown that Pi SLF is likely a component of a novel E3 ligase complex, which also contains Cullin-1 and a RING-HC protein, named Pi SBP1 (for *P. inflata* S-RNase Binding Protein1), a homolog of Ph

[1] Address correspondence to txk3@psu.edu.
The author responsible for distribution of materials integral to the findings presented in this article in accordance with the policy described in the Instructions for Authors (www.plantcell.org) is: Teh-hui Kao (txk3@psu.edu).
[W] Online version contains Web-only data.
www.plantcell.org/cgi/doi/10.1105/tpc.107.055426

(*P. hybrida*) SBP1 (Sims and Ordanic, 2001), but does not contain Skp1 or Rbx1 (RING-HC protein) (Hua and Kao, 2006). Since Pi SBP1 is approximately three times the size of Rbx1, it may play the roles of Skp1 and Rbx1. Whether this Pi SLF–containing complex is involved in mediating the ubiquitination and degradation of S-RNases in compatible pollen tubes remains to be determined. However, we have used cell-free systems to show that S-RNases are ubiquitinated and degraded in pollen tube extracts via the 26S proteasome pathway, although neither ubiquitination nor degradation was *S*-haplotype–specific (Hua and Kao, 2006). We have also used an in vitro binding assay to show that an allelic product of Pi *SLF* interacts with its non-self S-RNases more strongly than with its self S-RNase and that an S-RNase interacts with its non-self Pi SLFs more strongly than with its self Pi SLF (Hua and Kao, 2006). Thus, it is possible that a Pi SLF–containing complex specifically mediates the ubiquitination of non-self S-RNases in a pollen tube to target them for degradation.

F-box proteins constitute a large family of proteins in plants (e.g., the *Arabidopsis thaliana* genome encodes >700 F-box proteins) (Gagne et al., 2002; Risseeuw et al., 2003), and multiple F-box genes have been identified at the *S*-loci of all three families that possess S-RNase–based SI (McCubbin et al., 2000; Entani et al., 2003; Ushijima et al., 2003; Wang et al., 2003; Zhou et al., 2003; Sassa et al., 2007). The functions of none of these *S*-locus–linked *SLF*-like genes have been determined. Recently, Sassa et al. (2007) proposed that two highly similar F-box genes (87.5% identity in their deduced amino acid sequences) of apple (*Malus domestica*; Rosaceae), which are located at the *S*-locus, are specifically expressed in pollen, and show allelic polymorphism, may both encode the pollen specificity determinant.

In this work, we wished to examine whether Pi SLF is unique in its function in SI, and if so, which features of Pi SLF distinguish it from other F-box proteins that are similar in sequence and share other properties with Pi SLF. We first identified S_1- and/or S_2-alleles of four Pi *SLF-like* (Pi *SLFL*) genes and showed that at least three of them are tightly linked to the *S*-locus. We used an in vivo functional assay to show that none of these three *S*-locus–linked Pi *SLF*s controls pollen function in SI. We then used an in vitro binding assay to show that all four of the newly identified Pi SLFLs, as well as one of the two previously identified Pi SLFLs whose genes are linked to the *S*-locus (McCubbin et al., 2000; Wang et al., 2003), either failed to interact, or could not compete with Pi SLF_2 for interaction, with S_3-RNase (a non-self S-RNase for all of them). Comparison of the deduced amino acid sequences of three allelic variants of Pi SLF (Pi SLF_1, Pi SLF_2, and Pi SLF_3; Sijacic et al., 2004), the four newly identified Pi SLFLs, and the two previously identified Pi SLFLs revealed three Pi SLF–specific regions (SRs), named SR1, SR2, and SR3. We further divided Pi SLF_2 into three function domains (FDs), FD1, FD2, and FD3, which contain SR1, SR2, and SR3, respectively, and used in vitro binding assays to show that FD2, conserved among Pi SLF_1, Pi SLF_2, and Pi SLF_3, is primarily responsible for the strong interaction between an allelic product of Pi SLF and its non-self S-RNases. This interaction is negatively modulated by FD1 and FD3 and divergent among Pi SLFs, and the effect is much greater on self interactions than on non-self interactions between Pi SLF and S-RNase.

RESULTS

Isolation of Pi *SLFL* Genes from S_1 and S_2 Pollen cDNA Libraries of *P. inflata*

We were interested in identifying pollen-expressed F-box genes whose amino acid sequences share significant degrees of similarity with those of Pi *SLF* alleles outside the F-box domain. Thus, we used cDNA for Pi SLF_2(CTD) (340 amino acids), which does not contain the N-terminal 49 amino acids of the F-box domain, as a probe to screen previously constructed pollen cDNA libraries of S_1- and S_2-haplotypes (Skirpan et al., 2001). Under low-stringency hybridization conditions, six positive clones were obtained from screening 6×10^6 plaques of the S_1 cDNA library, and nine positive clones were obtained from screening 9×10^6 plaques of the S_2 cDNA library. Sequencing of all of these clones revealed that some of them corresponded to three previously identified genes: Pi *SLF* (Sijacic et al., 2004; Wang et al., 2004) and two *S*-locus–linked Pi *SLFL* genes, *A113* and *A134* (McCubbin et al., 2000; Wang et al., 2003). The remaining clones corresponded to four new genes based on their sequences and genomic DNA gel blotting (see next section). One class of cDNA clones identified from the S_1 library and one class of cDNA clones identified from the S_2 library were 93.7% identical in their coding sequences and 88.6% identical in their deduced amino acid sequences. Thus, they were considered allelic of the same gene and were named Pi *SLFLa*-S_1 and Pi *SLFLa*-S_2. The other classes of cDNA clones, one isolated from the S_1 library and two from the S_2 library, were 66.4 to 69.1% identical in their coding sequences, and they were designated Pi *SLFLb*-S_2, Pi *SLFLc*-S_1, and Pi *SLFLd*-S_2. The pairwise nucleotide sequence identities of these Pi *SLFL* genes and three alleles of Pi *SLF* are shown in Supplemental Table 1 online, and the pairwise sequence identities for their deduced amino acid sequences are shown in Supplemental Table 2 online. The Pi *SLFL* genes show 67.8 to 71.5% identity with the three Pi *SLF* alleles (Sijacic et al., 2004) in their coding sequences and 47.4 to 54.6% identity with these Pi *SLF* alleles in their deduced amino acid sequences.

Assessing Linkage of Four Pi *SLFL* Genes to the *S*-Locus

Genes that are linked to the *S*-locus typically show *S*-haplotype–specific sequence differences, and when they are used as probes in genomic DNA gel blot analysis they often show *S*-haplotype–specific restriction fragment length polymorphism (RFLP). Genomic DNA gel blotting was performed using the cDNAs for Pi *SLFLa*-S_1, Pi *SLFLa*-S_2, Pi *SLFLb*-S_2, Pi *SLFLc*-S_1, and Pi *SLFLd*-S_2 as probes. Pi *SLFLa*-S_1 and Pi *SLFLa*-S_2 showed the same monomorphic hybridization pattern (Figure 1A), confirming that they are allelic. Pi *SLFLb*-S_2, Pi *SLFLc*-S_1, and Pi *SLFLd*-S_2 corresponded to different genes, as they showed different *S*-haplotype–specific RFLPs (Figures 1B to 1D).

We next examined whether Pi *SLFLa*-S_2, Pi *SLFLb*-S_2, and Pi *SLFLd*-S_2 are located in an 881-kb contig containing *S_2-RNase* (Wang et al., 2004). We used PCR primers specific to each gene to separately amplify eight BAC clones that collectively span this contig. No DNA fragments were obtained for any of these three genes. Since *S_2-RNase* is located ~250 kb from the proximal

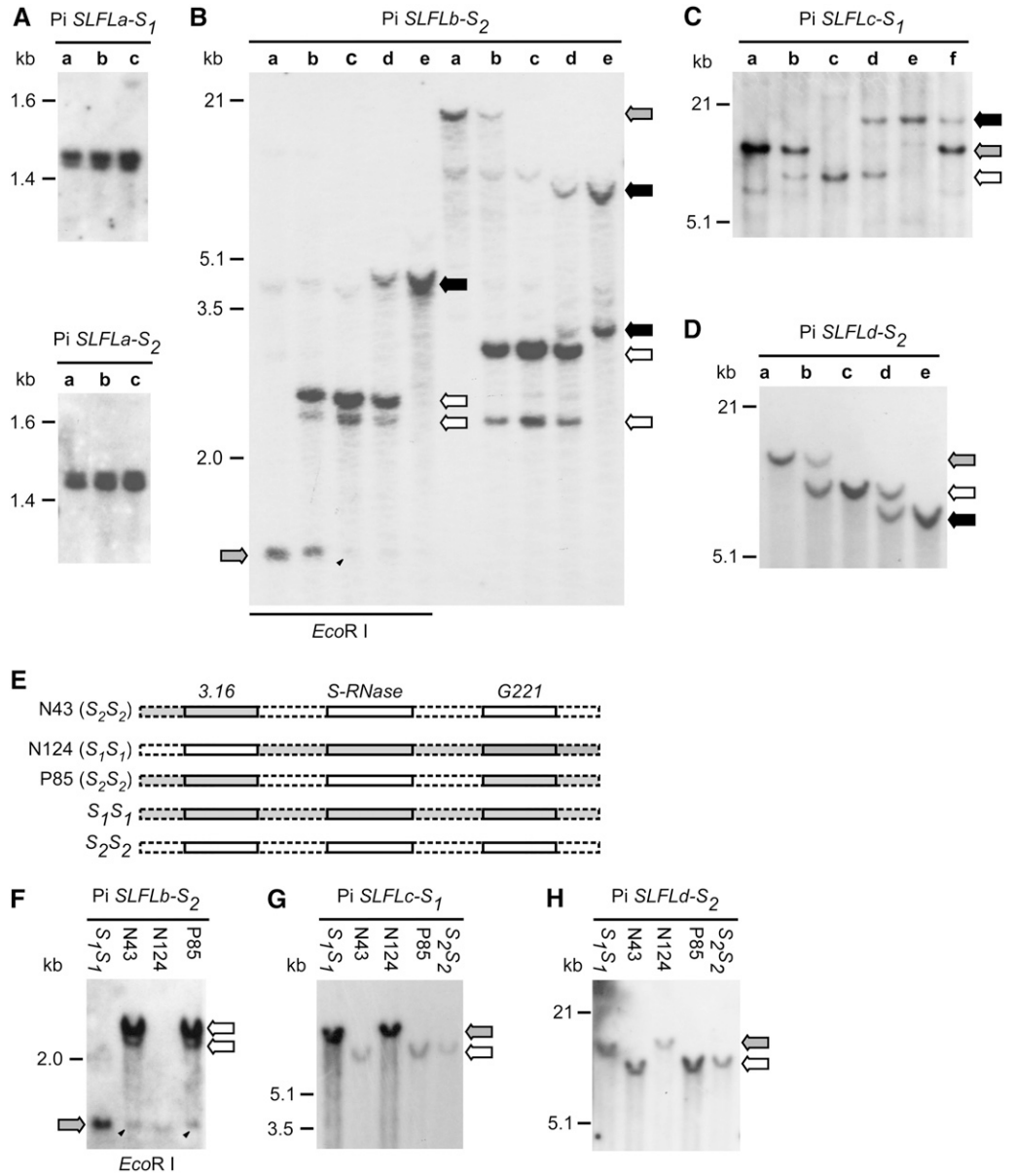

Figure 1. Genomic DNA Gel Blot Analysis of Pi *SLFL* Genes for *S*-Haplotype–Specific RFLP and Linkage to the *S*-Locus.

Genomic DNA (15 μg) isolated from each plant was digested with *Xba*I or *Eco*RI as indicated in **(B)** and **(F)**. The DNA digests were separated on 0.7% agarose gels. Each blot was hybridized with the ^{32}P-labeled cDNA probe indicated at the top of the autoradiogram at 65°C. The S_1-specific fragments are indicated with gray arrows, the S_2-specific fragments are indicated with white arrows, and the S_3-specific fragments are indicated with black arrows. For **(A)** to **(D)**, the *S* genotypes of the plants used are as follows: lane a, S_1S_1; lane b, S_1S_2; lane c, S_2S_2; lane d, S_2S_3; lane e, S_3S_3; lane f, S_1S_3. The arrowheads in **(B)** and **(F)** indicate a fragment that cross-hybridized with Pi *SLFLb*-S_2; this fragment is similar in size to the S_1-specific fragment of Pi *SLFLb* indicated with gray arrows.

(A) This blot was first hybridized with cDNA for Pi *SLFLa*-S_1; after autoradiography, the hybridized Pi *SLFLa*-S_1 probe was stripped off and the blot was rehybridized with cDNA for Pi *SLFLa*-S_2.

(B) to **(D)** Each blot was hybridized with the respective cDNA probe as indicated.

(E) Schematic representation of recombination between two markers, *3.16* and *G221*, and the *S-RNase* gene in three recombinant plants, N43, N124, and P85. S_1S_1 and S_2S_2 are wild-type plants. Chromosomal DNA of the S_1-haplotype is marked in gray, and that of the S_2-haplotype is marked in white. The *S* genotypes of the recombinant plants, determined by genomic blotting using *S-RNase* as a probe (Wang et al., 2003), are as follows: N43, S_2S_2; N124, S_1S_1; P85, S_2S_2.

(F) to **(H)** Each blot was hybridized with the respective cDNA probe as indicated.

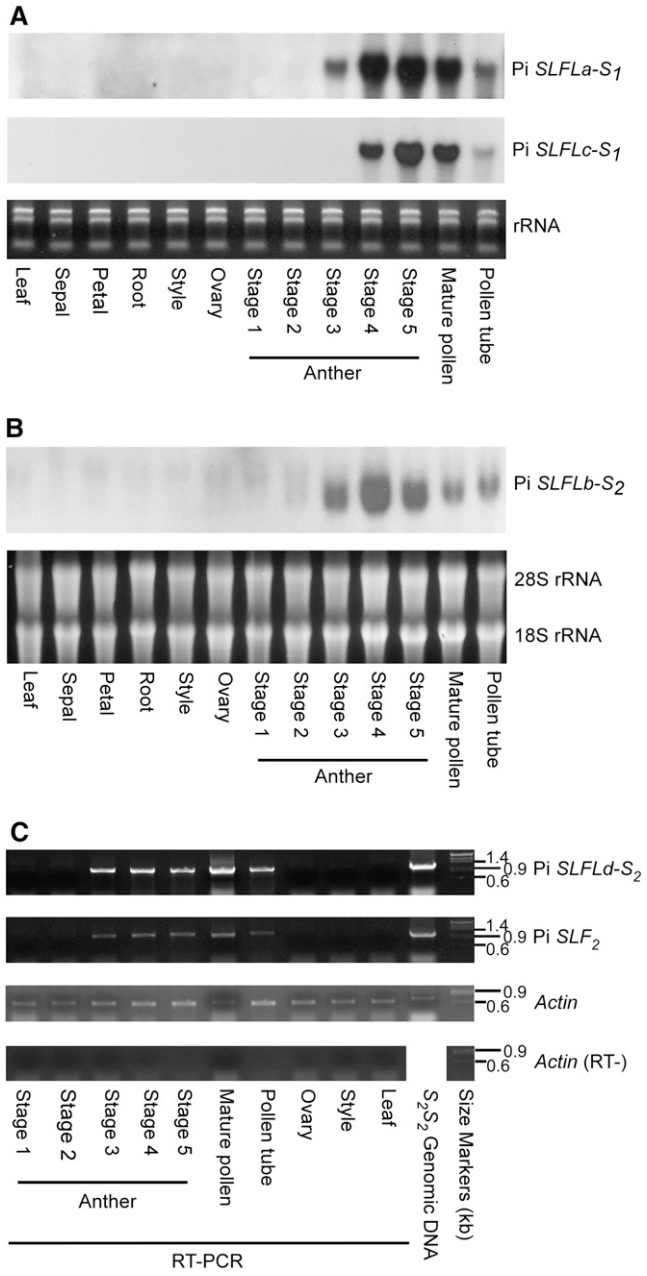

Figure 2. Expression Patterns of Four Pi *SLFL* Genes Determined by RNA Gel Blot or RT-PCR.

Total RNA was extracted from various tissues, and from anthers at five different developmental stages, of an S_1S_1 plant **(A)** and an S_2S_2 plant (**[B]** and **[C]**). Anther stages are defined by flower bud size as described by Lee et al. (1996).

(A) and **(B)** The RNA samples (10 μg/lane) were electrophoresed on 1.25% formamide-agarose gels, and each blot was hybridized with ^{32}P-labeled cDNA for one of the three Pi *SLFL* genes, as indicated. Equal loading of RNA samples was assessed by ethidium bromide staining of the rRNAs separated on a 1% agarose gel **(A)** or by ethidium bromide staining of the gel used in blotting **(B)**.

(C) RT-PCR products of Pi *SLFLd*-S_2 and Pi SLF_2 were electrophoresed on 1% agarose gels and visualized by ethidium bromide staining. To demonstrate equal amounts of RNA used for the amplification of Pi *SLFLd*-S_2 and Pi SLF_2, RT-PCR was performed on each RNA sample to amplify the *Actin* gene. To exclude contamination of genomic DNA in the RNA samples, RT-PCR was also performed using primers for the *Actin* gene on each sample in the absence of reverse transcriptase (RT−). PCR of genomic DNA of S_2S_2 genotype was used to demonstrate the size of the genomic DNA band.

end of the 881-kb contig, the results of PCR suggest that Pi *SLFLa*-S_2, Pi *SLFLb*-S_2, and Pi *SLFLd*-S_2 are located at least 250 kb away from S_2-*RNase*. By contrast, Pi SLF_2 is located within this contig, ~161 kb downstream of S_2-*RNase* (Wang et al., 2004). Since the *S*-locus region of *P. inflata*, where recombination is suppressed, exceeds 4.4 Mb (Wang et al., 2004), we further examined whether these genes could still be linked to the *S*-locus, but at greater distances from *S-RNase* than is Pi *SLF*.

We previously generated a population of 1205 F2 plants segregating for S_1- and S_2-haplotypes and used them to ascertain whether the genes identified from our search for *S*-linked pollen-expressed genes were tightly linked to the *S*-locus (Wang et al., 2003). Recombination was detected between some of the genes and *S-RNase* in nine F2 plants. The *S-RNase* gene and its flanking chromosomal regions in three of the recombinant plants are graphically shown in Figure 1E. In plants N43 (S_2S_2) and N124 (S_1S_1), recombination occurred between gene *3.16* and *S-RNase*, and in plant P85 (S_2S_2), a double crossover occurred, one between *3.16* and *S-RNase* and the other between *G221* and *S-RNase*. The genetic distances between these two marker genes, *3.16* and *G221*, and *S-RNase* are 0.17 and 0.08 centimorgan, respectively (Wang et al., 2003). To assess how tightly Pi *SLFLb*-S_2, Pi *SLFLc*-S_1, and Pi *SLFLd*-S_2 are linked to the *S*-locus, their cDNAs were used as probes in genomic blotting analysis of these three recombinant plants. Pi *SLFLa* was not included because it did not show *S*-specific RFLP (Figure 1A). All three Pi *SLFL* genes hybridized to their respective S_2-specific fragments in N43 and P85 and to their respective S_1-specific fragments in N124 (Figure 1F for Pi *SLFLb*-S_2, Figure 1G for Pi *SLFLc*-S_1, and Figure 1H for Pi *SLFLd*-S_2), consistent with the *S* genotypes of these three recombinant plants determined by the hybridization patterns of *S-RNase*. These results suggest that these three Pi *SLFL* genes lie within the *S*-locus region delimited by *3.16* and *G221* and are all tightly linked to *S-RNase*. Although we could not establish whether Pi *SLFLa* is tightly linked to the *S*-locus, since it is similar in sequence to Pi *SLF*, it was also included, along with the other three Pi *SLFL* genes, in the analyses described below.

Four Pi *SLFL* Genes Are Specifically Expressed in Pollen and Pollen Tubes

The RNA gel blotting results showed that Pi *SLFLa*-S_1, Pi *SLFLb*-S_2, and Pi *SLFLc*-S_1 were all expressed in pollen and in vitro germinated pollen tubes but not in any of the vegetative and female reproductive tissues examined (Figures 2A and 2B). During anther development, the transcripts of these genes were first detected in stage 3 anthers, reached the highest level in stage 4 and/or stage 5 anthers, and declined in mature pollen. The transcripts were also detected at low levels in pollen tubes.

The tissue-specific expression pattern and the expression pattern during anther development are similar to those of Pi *SLF* and two previously identified Pi *SLFL* genes, *A113* and *A134* (McCubbin et al., 2000; Sijacic et al., 2004). Furthermore, the results from RT-PCR showed that Pi *SLFLd-S_2*, like Pi *SLF_2*, was expressed in stages 3 to 5 anthers, pollen, and pollen tubes but not in stages 1 to 2 anthers, leaves, styles, or ovaries (Figure 2C).

Assessment of SI Function of Pi *SLFLb-S_2*, Pi *SLFLc-S_1*, and Pi *SLFLd-S_2*

We chose Pi *SLFLb-S_2*, Pi *SLFLc-S_1*, and Pi *SLFLd-S_2* to examine whether they control pollen function in SI. As stated above, these three genes share a similar tissue-specific expression pattern with Pi *SLF* (Figure 2) and they are also tightly linked to *S-RNase* (Figure 1), albeit at greater distances from *S-RNase* than Pi *SLF*. We used the same in vivo approach as that described by Sijacic et al. (2004) to ascertain whether Pi *SLFLb-S_2*, Pi *SLFLc-S_1*, and Pi *SLFLd-S_2* function in SI. This approach was based on the phenomenon, termed competitive interaction, that pollen carrying two different pollen *S*-alleles fails to function in SI (de Nettancourt, 2001). In our previous study of Pi *SLF*, we showed that expression of a Pi *SLF_2* transgene in pollen of *S_1S_1*, *S_1S_2*, and *S_2S_3* transgenic plants caused the breakdown of SI function in *S_1* and *S_3* pollen that carried the transgene (i.e., heteroallelic pollen) but not in *S_2* pollen that carried the transgene (i.e., homoallelic pollen).

In making the transgene constructs for Pi *SLFLb-S_2*, Pi *SLFLc-S_1*, and Pi *SLFLd-S_2*, we fused the coding sequence for a Green Fluorescent Protein (GFP) in-frame to the last codon of each gene and used a pollen-specific promoter of tomato (*Solanum lycopersicum*), *LAT52* (Twell et al., 1990), to express each transgene. The resulting transgene constructs, *pBI LAT52*-Pi *SLFLb-S_2:GFP*, *pBI LAT52*-Pi *SLFLc-S_1:GFP*, and *pBI LAT52*-Pi *SLFLd-S_2:GFP* (see Supplemental Figure 1 online), were introduced into *S_2S_3*, *S_1S_2*, and *S_2S_3* plants, respectively. The reason for using the *LAT52* promoter was because we had previously shown that pollen of *S_2S_3* transgenic plants carrying *LAT52*-Pi *SLF_2:GFP* produced strong GFP signals, whereas pollen of *S_2S_3* transgenic plants carrying the same Pi *SLF_2:GFP* coding sequence driven by the Pi *SLF_2* promoter did not produce any detectable signal. Thus, using the *LAT52* promoter would facilitate detection of the GFP fusion proteins by an anti-GFP antibody.

The transgenic plants that carried a single copy of *LAT52*-Pi *SLF_2:GFP*, *LAT52*-Pi *SLFLb-S_2:GFP*, *LAT52*-Pi *SLFLc-S_1:GFP*, or *LAT52*-Pi *SLFLd-S_2:GFP* were identified by genomic blotting. Pollen was collected from each single-copy transgenic plant, germinated in vitro, and examined for the expression of the GFP-fused protein. Those plants found to produce ~50% pollen tubes with GFP fluorescence were further analyzed by protein gel blotting using an anti-GFP antibody. Two plants each of the *LAT52*-Pi *SLF_2:GFP*, *LAT52*-Pi *SLFLb-S_2:GFP*, and *LAT52*-Pi *SLFLc-S_1:GFP* transgenic lines (Figure 3A) and four plants of the *LAT52*-Pi *SLFLd-S_2:GFP* transgenic line (Figure 3B) produced comparable levels of the GFP-fused proteins in pollen or stage 5 anthers. The results of genomic blotting for the 10 transgenic plants analyzed in Figure 3 are shown in Supplemental Figure 2 online.

The 10 transgenic plants mentioned above were further analyzed for their SI behavior. Both transgenic plants that carried *LAT52*-Pi *SLF_2:GFP* (named *S_2S_3*/Pi *SLF_2:GFP*-5 and -10; Figure 3A) showed the same SI behavior as the previously reported *S_2S_3* transgenic plants that expressed a single copy of the Pi *SLF_2* transgene (Sijacic et al., 2004). Both transgenic plants were completely self compatible, setting large-sized fruits with seed numbers comparable to those obtained from normally compatible pollinations. Moreover, their pollen was compatible with pistils of *S_2S_3* wild-type plants, but their pistils were incompatible with pollen of *S_2S_3* wild-type plants, suggesting that the pollen SI function, but not the pistil SI function, of these two transgenic plants was affected. We raised 41 plants from seeds obtained from pollination of a wild-type *S_2S_3* plant by *S_2S_3*/Pi *SLF_2:GFP*-5 and determined their *S* genotypes by PCR using primers specific to *S_2-RNase* and to *S_3-RNase*. The results from representative plants are shown in Figure 3C.

The *S_3-RNase*–specific fragment was detected in all 41 plants, and the *S_2-RNase*–specific fragment was detected in 22 of the 41 plants, indicating that 22 plants were of *S_2S_3* genotype and 19 were of *S_3S_3* genotype (in an ~1:1 ratio). The absence of progeny with the *S_2S_2* genotype suggests that both *S_2* pollen and *S_2* pollen carrying the transgene produced by *S_2S_3*/Pi *SLF_2:GFP*-5 functioned normally in SI and were rejected by the *S_2S_3* pistil. Furthermore, when pollen from each of the 41 progeny plants was germinated in vitro, ~50% of the pollen tubes produced by each plant were found to show GFP fluorescence by epifluorescence microscopy (the result of one progeny plant is shown in Supplemental Figure 3 online), suggesting that all of the progeny plants carried one copy of the transgene inherited from *S_2S_3*/Pi *SLF_2:GFP*-5. This finding, coupled with the finding that only *S_2S_2* and *S_2S_3* genotypes were present in the progeny, suggests that only the *S_3* pollen carrying the transgene was accepted by the wild-type *S_2S_3* pistil for fertilization. Thus, the expression of Pi *SLF_2:GFP* caused the breakdown of SI function in *S_3* pollen (heteroallelic pollen) but not in *S_2* pollen (homoallelic pollen). Similar results were obtained from the analysis of the progeny between a wild-type *S_2S_3* plant (female) and *S_2S_3*/Pi *SLF_2:GFP*-10 (male). We thus conclude that fusion of the GFP to the C terminus of Pi SLF_2 does not affect its function in SI.

In contrast with *S_2S_3*/Pi *SLF_2:GFP*-5 and -10, self-pollination of the two Pi *SLFLb-S_2* transgenic plants, the two Pi *SLFLc-S_1* transgenic plants, and the four Pi *SLFLd-S_2* transgenic plants analyzed in Figure 3 did not result in any fruit set (>10 pollinations for each transgenic plant). When we used pollen from each transgenic plant to pollinate wild-type plants with the same *S* genotype (e.g., pollen from *S_2S_3*/Pi *SLFLd-S_2:GFP*-30 was used to pollinate wild-type *S_2S_3* plants), no fruits were obtained either (>10 pollinations for each transgenic plant). To rule out the possibility that the Pi *SLFLb-S_2*, Pi *SLFLc-S_1*, and Pi *SLFLd-S_2* transgenes might have affected the function of pollen/pollen tubes produced by their respective transgenic plants, we performed crosses that were expected to be compatible with these transgenic plants (e.g., crosses between a wild-type *S_2S_3* plant [female] and *S_1S_2*/Pi *SLFLc-S_1:GFP*-20 [male]). Large-sized fruits characteristic of compatible pollination were obtained in all cases. We examined the inheritance of the transgene in each progeny by PCR analysis, using a primer specific to the transgene and a

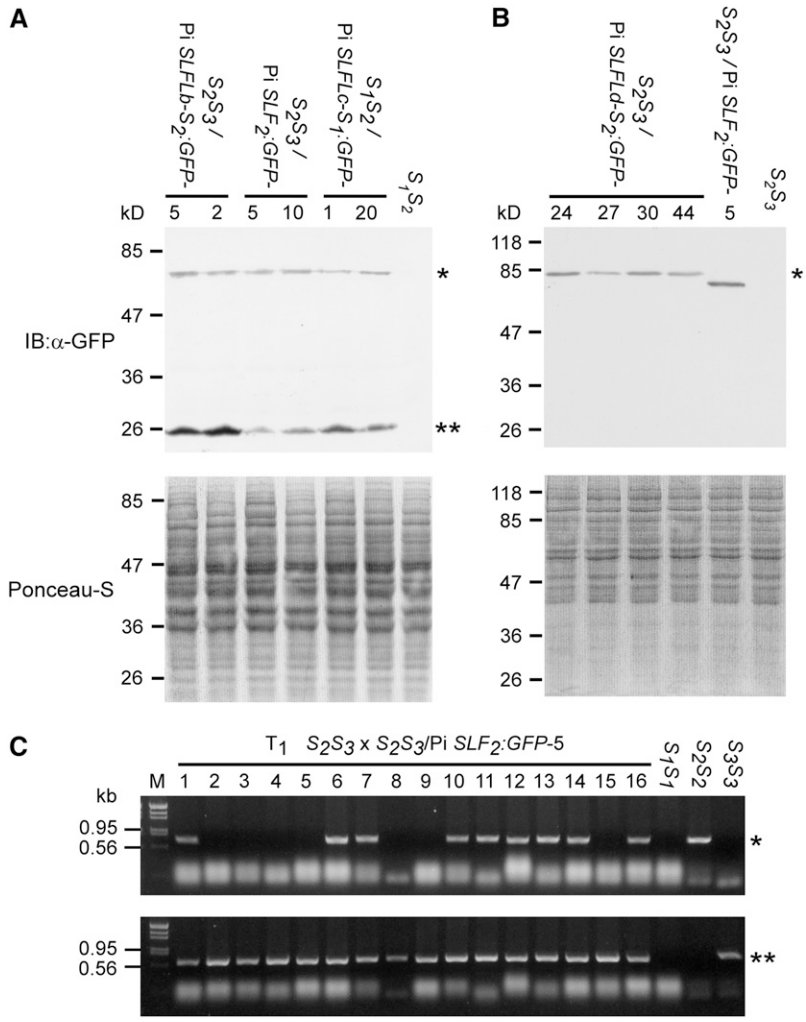

Figure 3. Functional Analysis of Three Pi *SLFL* Genes and Pi SLF_2 in Transgenic Plants.

(A) Protein gel blot showing that similar levels of proteins were produced from the Pi SLF_2*:GFP*, Pi *SLFLb-*S_2*:GFP*, and Pi *SLFLc-*S_1*:GFP* transgenes in six transgenic lines. Top panel, immunoblot (IB) of total pollen tube proteins. The single asterisk indicates Pi SLFLb-S_2:GFP, Pi SLF_2:GFP, or Pi SLFLc-S_1:GFP; the double asterisks indicate the cleaved GFP tag. Bottom panel, Ponceau S staining of the blot shown in the top panel before immunoblotting to reveal equal loading of total proteins.

(B) Protein gel blot showing that similar levels of proteins were produced from four independent Pi *SLFLd-*S_2*:GFP* plants and one Pi SLF_2*:GFP* plant. Top panel, immunoblot (IB) of total proteins from stage 5 anthers. The single asterisk indicates Pi SLFLd-S_2:GFP or Pi SLF_2:GFP. Bottom panel, Ponceau S staining of the blot shown in the top panel before immunoblotting to reveal equal loading of total proteins.

(C) PCR genotyping of the T1 progeny from pollination of a wild-type S_2S_3 plant by pollen of S_2S_3/Pi SLF_2*:GFP*-5. Genomic DNA (~500 ng) isolated from 16 progeny plants and from 3 wild-type plants (S_1S_1, S_2S_2, and S_3S_3) was amplified by primers specific to S_2*-RNase* (top panel) or S_3*-RNase* (bottom panel). The S_2*-RNase*–specific PCR fragment is indicated with a single asterisk, and the S_3*-RNase*-specific PCR fragment is indicated with double asterisks.

primer specific to the GFP coding sequence (see Supplemental Table 4 online for the primers used), and found that the transgene was transmitted to approximately half of the progeny. For example, of the 55 progeny plants from the pollination mentioned above, 27 were found to inherit the transgene. Thus, expression of Pi *SLFLb-*S_2, Pi *SLFLc-*S_1, and Pi *SLFLd-*S_2 in transgenic pollen did not affect the normal function of pollen/pollen tubes.

We further compared the extent of pollen tube growth in pistils of a wild-type S_2S_3 plant at 20 h after pollination by transgenic plants S_2S_3/Pi *SLFLd-*S_2*:GFP*-30 and S_2S_3/Pi *SLF-*S_2*:GFP*-5. For S_2S_3/Pi *SLFLd-*S_2*:GFP*-30, the growth of almost all pollen tubes was stopped in the upper segment of the pistil, similar to what was observed for pollination of the wild-type S_2S_3 plant by another wild-type S_2S_3 plant (see Supplemental Figures 4A and 4B online), whereas for S_2S_3/Pi *SLF-*S_2*:GFP*-5, almost all pollen tubes reached the bottom of the style, similar to what was observed for a compatible cross between the wild-type S_2S_3 plant and a wild-type S_1S_1 plant (see Supplemental Figures 4C and 4D online). These results further confirmed the SI behavior of the transgenic plants determined by the pollination experiments.

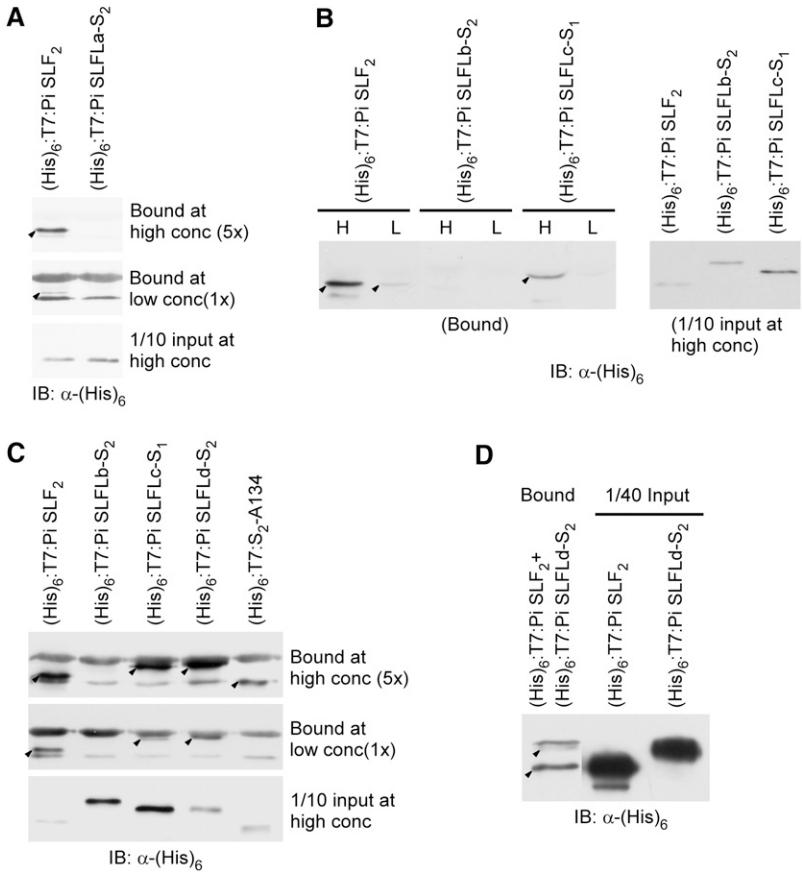

Figure 4. In Vitro Binding Assay for Interactions between Pi SLFL Proteins and S_3-RNase.

Pi SLFLa-S_2, Pi SLFLb-S_2, Pi SLFLc-S_1, Pi SLFLd-S_2, and S_2-A134 were expressed as $(His)_6$:T7-tagged proteins, and the purified proteins were incubated separately with GST:S_3-RNase–bound Glutathione Sepharose 4 Fast Flow beads. Pi SLF_2 was similarly expressed and purified for use as a control for binding to GST:S_3-RNase. The bound proteins were eluted and analyzed by immunoblotting (IB) using an anti-$(His)_6$ antibody. Each input lane contains one-tenth the amount of the $(His)_6$:T7-tagged protein used in the binding assay at the high concentration. The bound $(His)_6$:T7-tagged proteins are indicated with arrowheads. All of the other cross-reacting bands may correspond to *E. coli* proteins that copurified with the recombinant proteins used in the assay.

(A) Binding assay for Pi SLFLa-S_2.

(B) Binding assay for Pi SLFLb-S_2 and Pi SLFLc-S_1. H, binding assay performed at the high concentration of the indicated $(His)_6$:T7-tagged proteins; L, binding assay performed at the low concentration, which is one-fifth the high concentration.

(C) Binding assay for Pi SLFLb-S_2, Pi SLFLc-S_1, Pi SLFLd-S_2, and S_2-A134.

(D) Assay for competition between Pi SLF_2 and Pi SLFLd-S_2 for binding to GST:S_3-RNase. Equal amounts of $(His)_6$:T7:Pi SLF_2 and $(His)_6$:T7:Pi SLFLd-S_2 were incubated with GST:S_3-RNase in the same reaction. The amount of GST:S_3-RNase used was approximately one-twentieth that used in **(A)** to **(C)**.

Thus, all of the results together suggest that none of the three Pi *SLFL* genes examined caused the breakdown of SI function in heteroallelic pollen, and we conclude that Pi *SLFLb*, Pi *SLFLc*, and Pi *SLFLd* do not control pollen function in SI.

Analysis of Interactions between Pi SLFL Proteins and S_3-RNase by an in Vitro Binding Assay

We next examined whether the observation that Pi *SLFLb-S_2*, Pi *SLFLc-S_1*, and Pi *SLFLd-S_2* did not cause the breakdown of SI in heteroallelic pollen was due to the inability of these three Pi SLFLs to interact with S-RNases. We also included two other Pi SLFLs, Pi SLFLa-S_2 and S_2-A134, as well as Pi SLF_2 (as a control) in the binding assay. The other previously identified Pi SLFL, A113, was not included because there is no sequence difference between its S_1 and S_2 allelic variants. All of the F-box proteins used in the assay were expressed as $(His)_6$:T7-tagged proteins in *Escherichia coli*. The $(His)_6$:T7-tagged proteins were purified and assayed for interactions with glutathione *S*-transferase (GST):S_3-RNase, representing a non-self S-RNase for Pi SLF_2 and all of the Pi SLFLs tested. The amounts of GST:S_3-RNase bound to Glutathione Sepharose beads used in all of the binding reactions were in large excess over that of each $(His)_6$:T7-tagged protein to ensure that the binding was not limited by the amount of GST:S_3-RNase (see Supplemental Figure 5 online). After the binding reactions, the $(His)_6$:T7-tagged proteins were eluted and detected

by an anti-$(His)_6$ tag antibody. Since the amounts of the $(His)_6$:T7-tagged proteins used in the same assay were not the same, to compare their binding differences, the amount of each bound protein was normalized against the input amount (both of which were quantified by ImageQuant5.2).

Figure 4A shows the results of the binding assay for $(His)_6$:T7:Pi SLFLa-S_2 and $(His)_6$:T7:Pi SLF_2. Two different concentrations of these two proteins were used, and for each concentration, the amount of $(His)_6$:T7:Pi SLFLa-S_2 was approximately twice that of $(His)_6$:T7:Pi SLF_2. At the high concentration, $(His)_6$:T7:Pi SLF_2 interacted with GST:S_3-RNase, as expected; however, no binding was detected for $(His)_6$:T7:Pi SLFLa-S_2, even though its input amount was twice that of $(His)_6$:T7:Pi SLF_2. At the low concentration (20% of the high concentration), a weak binding could still be detected for $(His)_6$:T7:Pi SLF_2.

We performed a similar binding assay for $(His)_6$:T7:Pi SLFLb-S_2 and $(His)_6$:T7:Pi SLFLc-S_1. At each concentration, the amounts of $(His)_6$:T7:Pi SLFLb-S_2 and $(His)_6$:T7:Pi SLFLc-S_1 were 3 and 10 times, respectively, that of $(His)_6$:T7:Pi SLF_2. At the high concentration, no binding with GST:S_3-RNase was detected for $(His)_6$:T7:Pi SLFLb-S_2, whereas binding was detected for $(His)_6$:T7:Pi SLFLc-S_1, but the amount bound was much less than that detected for $(His)_6$:T7:Pi SLF_2, even though the amount of $(His)_6$:T7:Pi SLFLc-S_1 used in the assay was 10 times that of $(His)_6$:T7:Pi SLF_2 (Figure 4B). At the low concentration, a weak binding to GST:S_3-RNase could still be detected for $(His)_6$:T7:Pi SLF_2, but no detectable binding was observed for $(His)_6$:T7:Pi SLFLc-S_1 (Figure 4B). The interactions of $(His)_6$:T7:Pi SLFLb-S_2 and $(His)_6$:T7:Pi SLFLc-S_1 with GST:S_3-RNase were further examined along with $(His)_6$:T7:Pi SLFLd-S_2 and $(His)_6$:T7:S_2-A134, and the results are shown in Figure 4C. At each concentration, the amounts of $(His)_6$:T7:Pi SLFLb-S_2, $(His)_6$:T7:Pi SLFLc-S_1, $(His)_6$:T7:Pi SLFLd-S_2, and $(His)_6$:T7:S_2-A134 were ~30, 40, 8, and 5 times, respectively, that of $(His)_6$:T7:Pi SLF_2. At the high concentration, $(His)_6$:T7:Pi SLFLb-S_2, even at a higher relative amount to $(His)_6$:T7:Pi SLF_2 (30 to 1) than that used in the assay shown in Figure 4B (3 to 1), did not interact with GST:S_3-RNase. At a higher relative amount to $(His)_6$:T7:Pi SLF_2 (40 to 1) than that used in the assay shown in Figure 4B (10 to 1), the amount of $(His)_6$:T7:Pi SLFLc-S_1 bound to GST:S_3-RNase was similar to that detected for $(His)_6$:T7:Pi SLF_2 at the high concentration, but it was slightly less at the low concentration. At both high and low concentrations, the amounts of $(His)_6$:T7:Pi SLFLd-S_2 bound to GST:S_3-RNase were similar to the amounts of $(His)_6$:T7:Pi SLF_2 bound, even though the amount of $(His)_6$:T7:Pi SLFLd-S_2 used was eight times that of $(His)_6$:T7:Pi SLF_2 at each concentration. At the high concentration, the amount of $(His)_6$:T7:S_2-A134 bound to GST:S_3-RNase was approximately one-fifth that of $(His)_6$:T7:Pi SLF_2 bound, even though the amount of $(His)_6$:T7:S_2-A134 used in the assay was five times that of $(His)_6$:T7:Pi SLF_2. At the low concentration, no bound $(His)_6$:T7:S_2-A134 could be detected.

The results of the binding assays shown in Figures 4A to 4C indicate that (1) three of the five Pi SLFLs examined interact to varying extents with S_3-RNase, with $(His)_6$:T7:Pi SLFLd-S_2 interacting the strongest, and (2) all of these interactions are weaker than the interactions between Pi SLF_2 and S_3-RNase. To further confirm that Pi SLF_2 interacts with S_3-RNase much more strongly than does $(His)_6$:T7:Pi SLFLd-S_2, we performed a competition assay in a single reaction that contained equal amounts of $(His)_6$:T7:Pi SLF_2 and $(His)_6$:T7:Pi SLFLd-S_2 and an amount of GST:S_3-RNase that was one-twentieth that used in all of the other binding assays. A significantly larger amount of $(His)_6$:T7:Pi SLF_2 was bound to GST:S_3-RNase than $(His)_6$:T7:Pi SLFLd-S_2, confirming that Pi SLF_2 interacts with S_3-RNase much more strongly than does Pi SLFLd-S_2.

Sequence Comparison among Pi SLFs and Pi SLFLs

The deduced amino acid sequences of three alleles of Pi *SLF*, Pi *SLF_1*, Pi *SLF_2*, and Pi *SLF_3*, were aligned with those of Pi *SLFLa-S_1*, Pi *SLFLa-S_2*, Pi *SLFLb-S_2*, Pi *SLFLc-S_1*, Pi *SLFLd-S_2*, *S_1(S_2)-A113*, *S_3-A113*, *S_1-A134*, *S_2-A134*, and *S_3-A134* by ClustalW (Figure 5). To identify the regions that are specific to Pi SLF, we first used the sequence of Pi SLF_1 as a reference and compared each amino acid with the corresponding amino acid of each of the other sequences in the alignment (Figure 5). An index number (-1 or $+1$) was assigned to the amino acid of the sequence being compared with Pi SLF_1 if it was identical to or different from the reference amino acid of Pi SLF_1. After all of the sequences had been compared with the Pi SLF_1 sequence, the index numbers for each site of the alignment were summed to obtain the index value for that site. A sliding window analysis of the index value was then performed (using a window of 60 sites and a 6-site slide), and the value for each window was plotted against the starting site of that window. The process was repeated using Pi SLF_2 and then Pi SLF_3 as a reference sequence. The plots for these three allelic variants of Pi SLF are very similar, and they all contain three major peaks (Figure 6A). The regions delimited by these three peaks represent Pi SLF–specific regions, and they were named SR1 (sites 62 to 114), SR2 (sites 184 to 196), and SR3 (sites 268 to 305) (Figure 5). Secondary structure predictions revealed that all three regions contained loop structures (Figure 5), which could potentially be involved in protein–protein interactions.

We next analyzed the amino acid sequences of Pi SLF_1, Pi SLF_2, and Pi SLF_3 (see the alignment in Supplemental Figure 6 online) using the normed variability index (Kheyr-Pour et al., 1990) to identify the most divergent regions (Figure 6B). Two regions, named Va and Vb (for variable a and variable b, respectively), were identified, and interestingly, they are contained within SR1 and SR3, respectively (see Supplemental Figure 6 online). To examine whether the Va and Vb regions are under positive selection during evolution, the ratios of Ka (nonsynonymous nucleotide substitutions) to Ks (synonymous nucleotide substitutions) were calculated for each pairwise comparison of the coding sequences of these three alleles of Pi *SLF* (Figure 6C). The results show that the nucleotide sequence for the Va region is possibly under positive selection.

Dissecting the Biochemical Functions of Three Different Regions of Pi SLF_2

Based on the three Pi SLF–specific regions (Figures 5 and 6) and preliminary biochemical characterization of the GST:S_3-RNase binding properties of 11 truncated forms of Pi SLF_2 (see Supplemental Table 3 online), we divided Pi SLF_2 into three functional

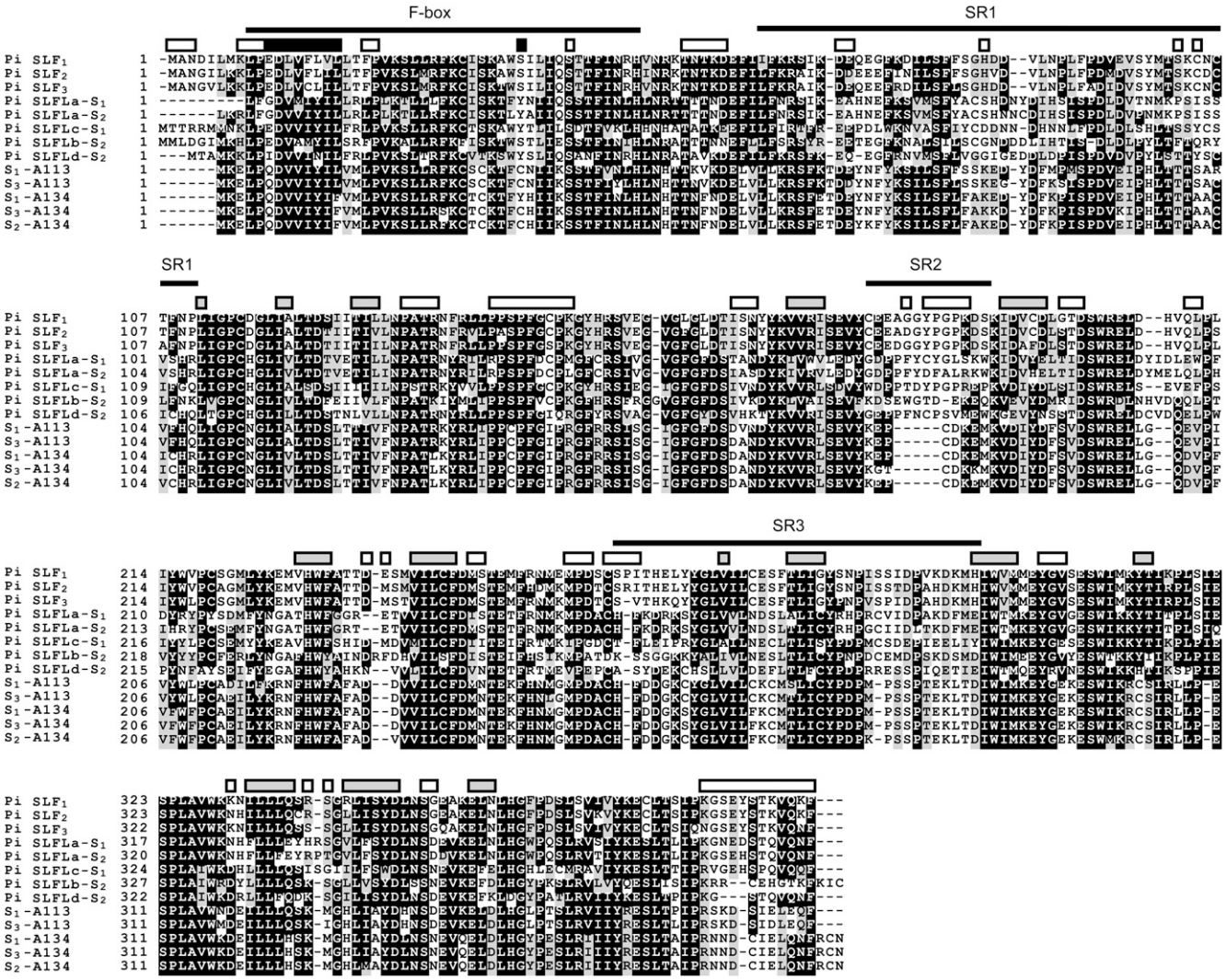

Figure 5. Alignment of the Deduced Amino Acid Sequences of Three Alleles of Pi *SLFs* and Six Pi *SLFL* Genes (Some with Multiple Alleles).

Amino acids that are conserved at a given site are highlighted in black shading; amino acids that are similar to the conserved residues are highlighted in gray shading. The regions of Pi SLF_1 predicted by the PROFsec program (http://cubic.bioc.columbia.edu/predictprotein/) to assume α-helix, β-sheet, and loop secondary structures (with >82% of the expected average accuracy) are indicated by black, gray, and white bars, respectively. The F-box domain predicted by SMART (http://smart.embl-heidelberg.de/smart/set_mode.cgi?NORMAL=1) and the three Pi SLF–specific regions, SR1, SR2, and SR3, are indicated by black lines above the aligned sequences.

domains, named FD1, FD2, and FD3, which contain SR1, SR2, and SR3, respectively (Figure 7A; see Supplemental Figure 6 online). We then generated five $(His)_6$:T7-tagged truncated constructs, each containing one or two of the FDs. All except the construct containing FD1 alone were successfully expressed in *E. coli*. Each $(His)_6$:T7-tagged protein was purified and tested for interactions with GST:S_3-RNase, as described in the previous section.

Both $(His)_6$:T7:Pi SLF_2(FD2) and $(His)_6$:T7:Pi SLF_2(FD3) interacted with GST:S_3-RNase; however, FD2 interacted more strongly than did FD3 and, most notably, even more strongly than did the full-length protein (cf. lanes b, c, and f in Figure 7B and bars b, c, and f in Figure 7C). FD2+FD3 interacted with GST:S_3-RNase to a lesser extent than did FD2 alone (cf. lanes b and e in Figure 7B and bars b and e in Figure 7C), but still to a greater extent than did the full-length protein (cf. lanes e and f in Figure 7B and bars e and f in Figure 7C). Finally, FD1+FD2 interacted with GST:S_3-RNase less strongly than did FD2 alone and FD2+FD3 (cf. lanes b, d, and e in Figure 7B and bars b, d, and e in Figure 7C), but more strongly than did the full-length protein (cf. lanes d and f in Figure 7B and bars d and f in Figure 7C). All of these results together suggest that (1) FD2 of Pi SLF_2 is the primary region for interactions with S_3-RNase, and (2) the interactions between FD2 and S_3-RNase may be negatively modulated by FD1 and FD3, with FD1 exerting a greater effect.

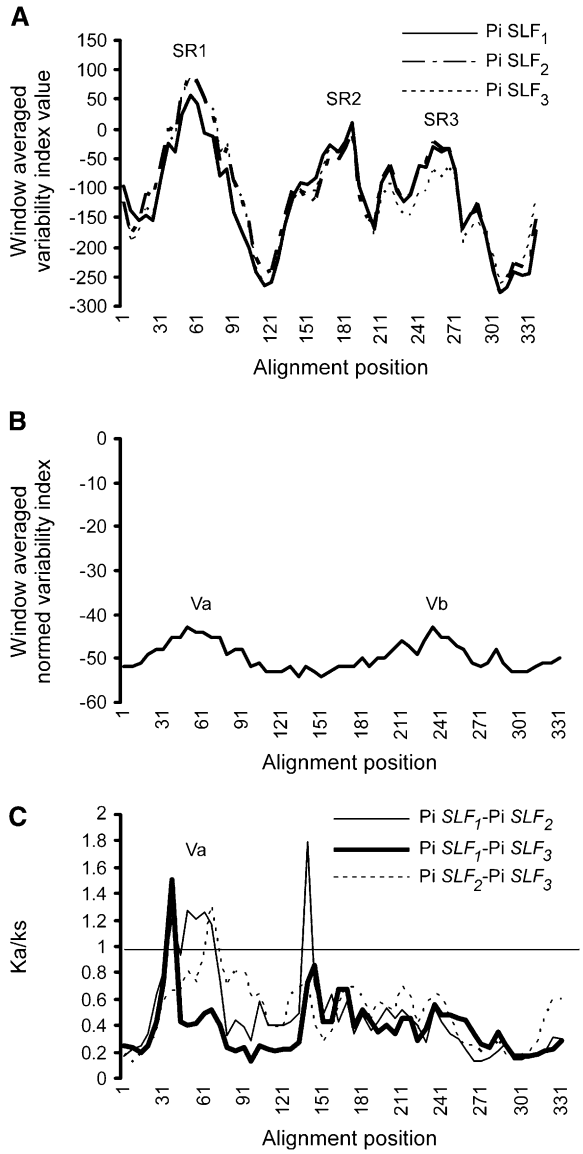

Figure 6. Sequence Analysis of Pi SLF and Pi SLFL Proteins.

(A) Plots of window-averaged variability index values calculated using Pi SLF_1, Pi SLF_2, and Pi SLF_3 as reference sequences. The alignment in Figure 5 was used for sequence comparison between each allelic variant of Pi SLF and all of the Pi SLFL sequences. The window-averaged variability index value for each site of the alignment was obtained by a sliding-window analysis (using a 60–amino acid window and a 6–amino acid slide), as described in the text. The peaks, named SR1, SR2, and SR3, represent Pi SLF–specific regions.

(B) Plot of the window-averaged norm variability index calculated based on the alignment of the amino acid sequences of Pi SLF_1, Pi SLF_2, and Pi SLF_3 shown in Supplemental Figure 6 online. The index for each sliding window (60–amino acid window and 6–amino acid slide) was calculated according to the method of Kheyr-Pour et al. (1990). The peaks, named Va and Vb, represent two regions of variability among the three Pi SLFs.

(C) Plots of Ka/Ks calculated based on pairwise comparison of the nucleotide sequences of Pi SLF_1, Pi SLF_2, and Pi SLF_3. A sliding window was used at a 180-bp window and an 18-bp slide. The numbers refer to amino acid residues as shown in **(B)**.

Contribution of FD2 of Pi SLF_2 to Strong Interactions with a Non-Self S-RNase

FD2 of Pi SLF_2 [Pi SLF_2(FD2)] contains SR2, one of the three Pi SLF–specific regions (Figures 5 and 6A; see Supplemental Figure 6 online), and the results of the binding assay shown in Figure 7 suggest that FD2 is the primary region for interaction with S_3-RNase, a non-self S-RNase of Pi SLF_2. Thus, we further examined the role of Pi SLF_2(FD2) by a domain-swapping approach. Since Pi SLFLb-S_2 did not interact with S_3-RNase (Figures 4B and 4C), we swapped FD2 of Pi SLF_2 and the corresponding domain of Pi SLFLb-S_2 to generate two $(His)_6$:T7-tagged chimeric proteins, $(His)_6$:T7:Pi SLF_2(FD1):Pi SLFLb-S_2(FD2):Pi SLF_2(FD3) and $(His)_6$:T7:Pi SLFLb-S_2(FD1):Pi SLF_2(FD2):Pi SLFLb-S_2(FD3) (Figure 8A). We then determined whether these two chimeric proteins could interact with GST:S_3-RNase, and if so, what effect the domain swapping had on the binding properties of Pi SLF_2 and Pi SLFLb-S_2. Similar to what was observed previously, $(His)_6$:T7:Pi SLF_2 interacted strongly with GST:S_3-RNase, but there was no detectable interaction between $(His)_6$:T7:Pi SLFLb-S_2 and GST:S_3-RNase (Figures 8B, lanes a and b, and 8C, bars a and b). Replacing FD2 of Pi SLF_2 with the corresponding domain of $(His)_6$:T7:Pi SLFLb-S_2 greatly reduced the extent of interactions with GST:S_3-RNase (cf. lanes a and c in Figure 8B and bars a and c in Figure 8C). Most interestingly, replacing the corresponding FD2 of Pi SLFLb-S_2 with FD2 of Pi SLF_2 conferred on the chimeric Pi SLFLb-S_2 the ability to interact with GST:S_3-RNase (cf. lanes b and d in Figure 8B and bars b and d in Figure 8C). All of these results confirm that FD2 of Pi SLF_2 plays an important role in the interactions with S_3-RNase. However, the findings that the chimeric Pi SLF_2 could still interact with GST:S_3-RNase (Figures 8B, lane c, and 8C, bar c) and that FD3 alone could interact with S_3-RNase (Figures 7B, lane c, and 7C, bar c) suggest that some amino acids in FD3 also contribute to the interactions.

FD1 and FD3 Together Determine the Specificity of Pi SLF in Its Interaction with S-RNase

The results of the binding assay for the full-size Pi SLF_2 and its various truncated forms showed that addition of FD1 or FD3 to FD2 reduced the interaction between FD2 and S_3-RNase (Figures 7B and 7C). Moreover, sequence comparison among three allelic variants of Pi SLF revealed that FD1 and FD3 each contained one of the two variable regions of Pi SLF (Figure 6B; see Supplemental Figure 6 online). Thus, we hypothesized that FD1 and FD3 might differentially control the interactions between a Pi SLF and its self and non-self S-RNases through blocking the interactions between FD2 and S-RNases more strongly under self interactions than under non-self interactions. That is, FD1 and FD3 might determine the allelic specificity of Pi SLF such that the interactions between matching specificity determinants of Pi SLF and S-RNase would significantly weaken the general interactions between FD2 and S-RNase. To examine this possibility, we made four constructs to express chimeric proteins between Pi SLF_1 and Pi SLF_2 by swapping either FD1 alone or both FD1 and FD3 (Figures 9A and 9D) and assessed the effects of the domain swapping on the interactions

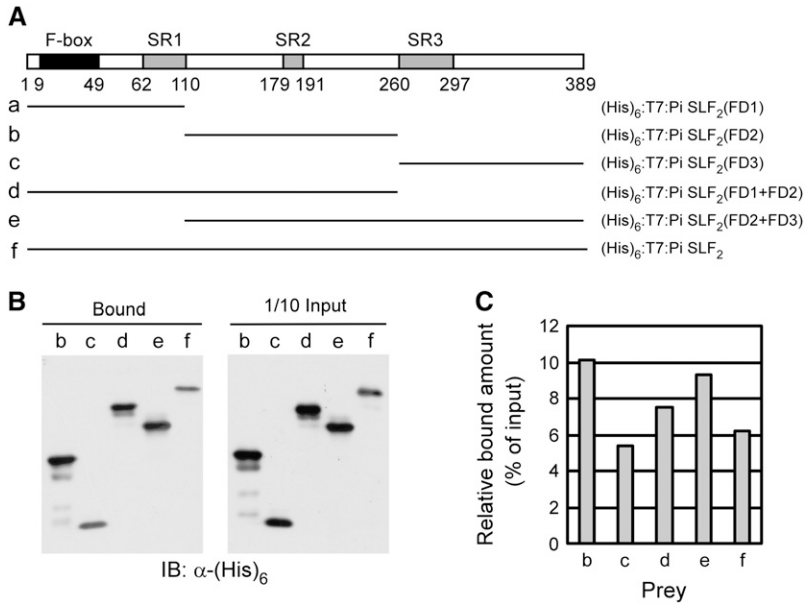

Figure 7. Roles of Three Separate Regions of Pi SLF_2 in Its Interactions with S_3-RNase.

(A) Schematic representation of five truncated versions of Pi SLF_2 and the full-length protein. Each was expressed as a $(His)_6$:T7-tagged protein in *E. coli*. The amino acid residues that demarcate the F-box domain and the three Pi SLF–specific regions, SR1, SR2, and SR3, are indicated.

(B) In vitro assay for interactions between GST:S_3-RNase and five $(His)_6$:T7-tagged truncated Pi SLF_2 proteins and the full-length Pi SLF_2. The assay was performed as described in the legend to Figure 4.

(C) Quantification of the binding results shown in **(B)**. The intensity of each bound band as well as the input band was quantified by ImageQuant5.2 (GE Healthcare). The relative bound amount for each $(His)_6$:T7-tagged protein used in the assay was calculated as the percentage of the total input amount.

of Pi SLF_1 and Pi SLF_2 with S_2-RNase under both non-self and self-interaction conditions.

Consistent with our previous finding that a Pi SLF interacted with its non-self S-RNases much more strongly than with its self S-RNase (Hua and Kao, 2006), Pi SLF_1 interacted much more strongly with S_2-RNase than did Pi SLF_2 (cf. lanes a and b in Figures 9B and 9E and bars a and b in Figures 9C and 9F). When FD1 of Pi SLF_2 was replaced with FD1 of Pi SLF_1, the chimeric protein interacted with S_2-RNase much more strongly than did Pi SLF_2 (cf. lanes b and c in Figure 9B and bars b and c in Figure 9C). One interpretation of this finding is that the negative effect of FD1 of Pi SLF_2 on the self interaction between Pi SLF_2 and S_2-RNase was alleviated when this FD1 was replaced with FD1 of Pi SLF_1, a non-self Pi SLF for S_2-RNase. When FD1 of Pi SLF_1 was replaced with FD1 of Pi SLF_2, the chimeric protein still interacted with S_2-RNase to a similar extent as did Pi SLF_1 (cf. lanes a and d in Figure 9B and bars a and d in Figure 9C), suggesting that FD1 alone is not sufficient to negatively regulate the strong general interactions between FD2 of a Pi SLF and its self S-RNase and that FD3 may cooperate with FD1 in this regulatory function.

Indeed, when both FD1 and FD3 of Pi SLF_1 were replaced with the corresponding domains of Pi SLF_2, the chimeric protein behaved like Pi SLF_2 in that its interaction with S_2-RNase was as weak as the self interaction between Pi SLF_2 and S_2-RNase (cf. lanes b and f in Figure 9E and bars b and f in Figure 9F). Conversely, when FD1 and FD3 of Pi SLF_2 were replaced with the corresponding regions of Pi SLF_1, the chimeric protein behaved like Pi SLF_1 in that it interacted with S_2-RNase to a similar extent as the non-self interaction between Pi SLF_1 and S_2-RNase (cf. lanes a and e in Figure 9E and bars a and e in Figure 9F). These results also suggest that FD2 is unlikely to contribute to the specific interaction between Pi SLF and S-RNase, because the chimeric Pi SLF_1 protein, containing FD2 of Pi SLF_2 (Figure 9D, bar e), still retained the strong binding affinity of Pi SLF_1 for S_2-RNase (i.e., non-self interactions; compare lanes a and e in Figure 9E and bars a and e in Figure 9F). Moreover, the chimeric Pi SLF_2, containing FD2 of Pi SLF_1 (Figure 9D, bar f), still interacted with S_2-RNase as weakly as did Pi SLF_2 (i.e., self interactions; compare lanes b and f in Figure 9E and bars b and f in Figure 9F).

DISCUSSION

In this work, we have identified four F-box genes of *P. inflata*, Pi *SLFLa*, Pi *SLFLb*, Pi *SLFLc*, and Pi *SLFLd*, which share several properties with Pi *SLF*. Their deduced amino acid sequences are similar to those of three alleles of Pi *SLF* that we studied previously (e.g., 47.6 to 54.4% identical to Pi SLF_2; see Supplemental Table 2 online); they are specifically expressed in pollen/pollen tubes; all except Pi *SLFLa* show *S*-haplotype–specific RFLP and have been shown to be tightly linked to the *S*-locus. We have used these four Pi *SLFL* genes, along with the two previously identified *S*-locus–linked Pi *SLFL* genes, A113 and A134, to investigate whether Pi *SLF* is unique in its function in SI and, if so, which properties/features of Pi SLF confer on it the unique function.

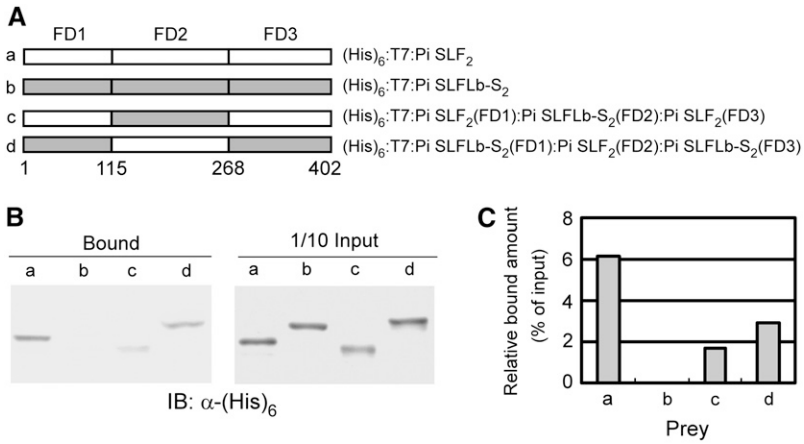

Figure 8. Analysis of the Biochemical Function of FD2 of Pi SLF_2 by Domain Swapping.

(A) Schematic representation of $(His)_6$:T7:Pi SLF_2, $(His)_6$:T7:Pi SLFLb-S_2, and their two chimeric proteins with the FD2 region swapped between them. The numbers demarcating FD1, FD2, and FD3 refer to the amino acid alignment sites (see Figure 5 for actual amino acid residues).
(B) In vitro binding assay for the interaction of $(His)_6$:T7:Pi SLF_2, $(His)_6$:T7:Pi SLFLb-S_2, and the two chimeric proteins with GST:S_3-RNase. The binding assay was performed as described in the legend to Figure 4.
(C) Quantification of the binding results shown in **(B)**. The quantification was performed as described in the legend to Figure 7C.

We used the same approach that we used previously to establish the function of Pi *SLF* in SI to examine whether three of the four Pi *SLFL* genes identified in this work, Pi *SLFLb*, Pi *SLFLc*, and Pi *SLFLd*, play a similar role in SI. We first used *LAT52:*Pi *SLF_2:GFP* as a control to show that fusion of GFP to the C-terminal end of Pi SLF_2 did not affect its function in SI. That is, expression of Pi *SLF_2:GFP* in S_2S_3 transgenic plants caused the breakdown of SI function in S_3 pollen carrying the transgene (heteroallelic pollen) but not in S_2 pollen carrying the transgene (homoallelic pollen), the same results that were obtained previously with Pi *SLF_2* (Sijacic et al., 2004). We then showed that Pi *SLFLb-S_2:GFP*, Pi *SLFLc-S_1:GFP*, and Pi *SLFLd-S_2:GFP* did not cause the breakdown of SI function in heteroallelic pollen, even though their proteins were produced to comparable levels in respective transgenic plants as the protein produced from Pi *SLF_2:GFP* in the control S_2S_3 transgenic plants. Thus, none of these three Pi *SLFL* genes plays a role in the *S*-specificity of pollen.

All of the earlier models of the S-RNase–based SI mechanism, proposed prior to the identification of the pollen *S* gene, predicted that the interactions of an allelic product of the pollen *S* gene with its self S-RNase were thermodynamically favored over the interactions with its non-self S-RNases (for review, see Kao and Tsukamoto, 2004). This prediction was based on the assumption that (1) self interactions are through the matching allele-specific domains of a pollen *S*-allele product and its self S-RNase, whereas non-self interactions are through a domain common to all pollen *S*-allele products and a domain common to all S-RNases; and (2) evolution of the SI mechanism has selected for matching allelic products of the male and female *S* genes to recognize and interact with each other. Since the outcome of self interactions in SI is inhibition of pollen tube growth, these models also predict that self interactions between the allele-specific domains render self S-RNase immune to inhibition either by the RNase inhibition domain of the matching pollen *S*-allele product (Kao and Tsukamoto, 2004) or by a general RNase inhibitor (Luu et al., 2001; see below).

After the pollen *S* gene was identified, these earlier models were modified to take into account the potential function of SLF/SFB in mediating the ubiquitination and degradation of S-RNases (Qiao et al., 2004a; Sijacic et al., 2004; Hua and Kao, 2006). That is, self interactions would result in the inability of self S-RNase to be ubiquitinated and degraded, whereas non-self interactions would result in the ubiquitination and degradation of non-self S-RNases. However, if self interaction is thermodynamically favored over non-self interaction, and if self interactions result in the protection of self S-RNase from being degraded, these predictions cannot explain the phenomenon of competitive interaction. For example, if a heteroallelic pollen tube producing both Pi SLF_1 and Pi SLF_2 has penetrated into an S_1S_2 pistil and taken up S_1- and S_2-RNases, Pi SLF_1 would preferentially interact with S_1-RNase and Pi SLF_2 would preferentially interact with S_2-RNase. As a result, neither S_1-RNase nor S_2-RNase would be degraded; thus, they would inhibit the growth of this heteroallelic pollen tube. This predicted outcome is precisely the opposite of what is observed. This conundrum led Luu et al. (2001) to propose a general inhibitor model. They hypothesized that a pollen *S*-allele product forms a homotetramer, which interacts with its self S-RNase and protects it from inhibition by a general RNase inhibitor. Using the example of heteroallelic pollen given above, Pi SLF_1 and Pi SLF_2 would form a heterotetramer, which would be unable to interact with either S_1-RNase or S_2-RNase. As a result, both S-RNases would be inhibited by the general RNase inhibitor, and this heteroallelic pollen tube would be compatible with S_1S_2 pistils. However, no biochemical data supporting this model have been reported yet.

We recently used an in vitro binding assay to compare the interactions of an allelic product of Pi *SLF* with its self and

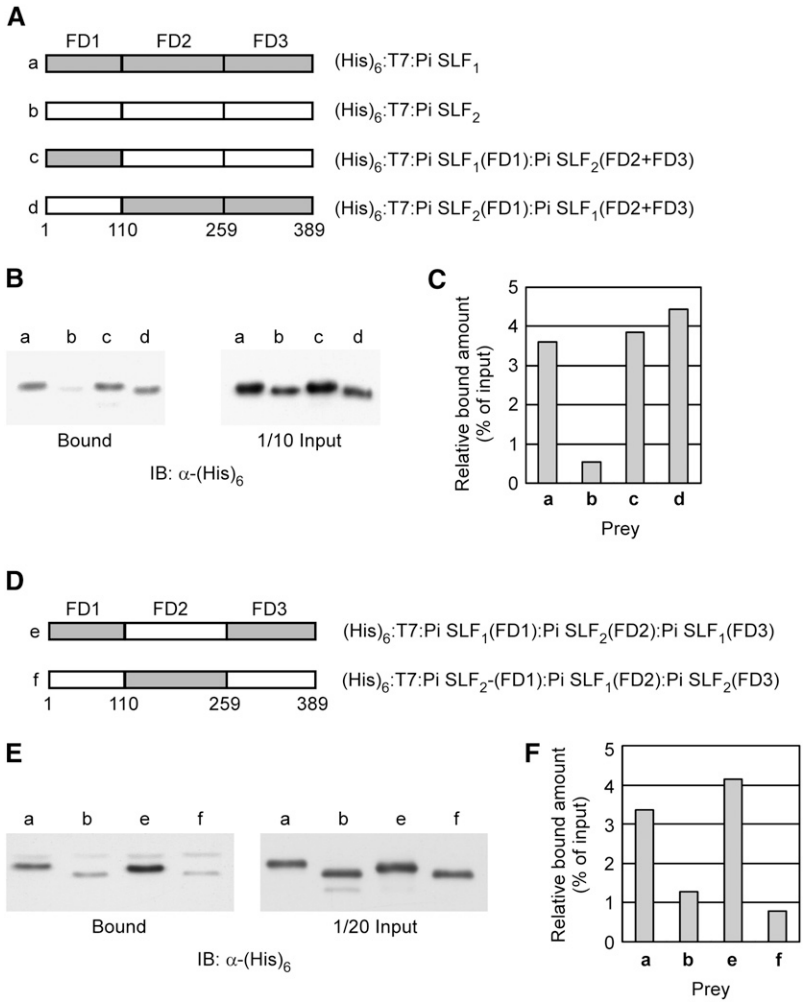

Figure 9. Analysis of the Biochemical Functions of FD1 and FD3 of Pi SLF_2 by Domain Swapping.

(A) Schematic representation of $(His)_6$:T7:Pi SLF_1, $(His)_6$:T7:Pi SLF_2, and the two chimeric proteins with the FD1 region swapped between them. The amino acid residue numbers demarcating FD1, FD2, and FD3 are shown (see Supplemental Figure 6 online for actual amino acid residues).

(B) In vitro binding assay for the interaction of GST:S_2-RNase with $(His)_6$:T7:Pi SLF_1, $(His)_6$:T7:Pi SLF_2, and the two chimeric proteins shown in **(A)**. The binding assay was performed as described in the legend to Figure 4.

(C) Quantification of the binding results shown in **(B)**. The quantification was performed as described in the legend to Figure 7C.

(D) Schematic representation of two chimeric proteins with FD1 and FD3 swapped between $(His)_6$:T7:Pi SLF_1 and $(His)_6$:T7:Pi SLF_2. The amino acid residue numbers are as shown in **(A)**.

(E) In vitro binding assay for the interaction of $(His)_6$:T7:Pi SLF_1, $(His)_6$:T7:Pi SLF_2, and the two chimeric proteins from **(D)** with GST:S_2-RNase. The binding assay was performed as described in the legend to Figure 4.

(F) Quantification of the binding results shown in **(E)**. The quantification was performed as described in the legend to Figure 7C.

non-self S-RNases and the interactions of an S-RNase with its self and non-self Pi SLFs (Hua and Kao, 2006). Contrary to our previous prediction, we found that a Pi SLF interacted with its non-self S-RNases more strongly than with its self S-RNase, and similarly, that an S-RNase interacted with its non-self Pi SLFs more strongly than with its self Pi SLF. This unexpected finding provides an explanation for competitive interaction. Again, using the example given above, Pi SLF_1 would preferentially interact with S_2-RNase and Pi SLF_2 would preferentially interact with S_1-RNase to mediate their degradation (see Figure 9C in Hua and Kao, 2006). If there is any Pi SLF_1 or Pi SLF_2 molecule that binds its self S-RNase, the complex might rapidly dissociate, because self interactions are much weaker than non-self interactions, allowing the dissociated S-RNase to bind its non-self Pi SLF and be degraded. As a result, both S_1- and S_2-RNases would be degraded and this heteroallelic pollen tube would be accepted by the S_1S_2 pistil.

Our model for the biochemical basis of competitive interaction, and SI interactions in general, is further supported by the in vitro binding results of Pi SLFLb-S_2, Pi SLFLc-S_1, and Pi SLFLd-S_2

(Figures 4B to 4D). For example, when Pi *SLFLb-S_2* was introduced into S_2S_3 plants, the heteroallelic pollen produced Pi SLF_3 and Pi SLFLb-S_2. Pi SLF_3 would mediate the degradation of S_2-RNase, but Pi SLFLb-S_2 would not be able to mediate the degradation of S_3-RNase, because it does not interact with S_3-RNase (Figures 4B and 4C). As a result, Pi *SLFLb-S_2* would not alter the SI behavior of heteroallelic pollen produced by S_2S_3 transgenic plants, which was precisely what we observed. All of the Pi SLFLs examined in this work either failed to interact with S_3-RNase (i.e., Pi SLFLa-S_2 and Pi SLFLb-S_2; Figures 4A to 4C) or interacted with S_3-RNase much more weakly than did Pi SLF_2 (i.e., Pi SLFLc-S_1, Pi SLFLd-S_2, and S_2-A134; Figures 4B to 4D). Thus, under the normal situation in which pollen only carries a single allele of Pi *SLF*, none of these Pi SLFLs would be able to compete with this allelic product of Pi SLF for binding to any of its non-self S-RNases.

We further investigated our hypothesis that the unique function of Pi *SLF* in SI is due in large part to the fact that it has coevolved with *S-RNase* to allow their allelic products to interact more strongly between nonmatching alleles than between matching alleles. We first identified three Pi SLF–specific regions, SR1, SR2, and SR3, which are divergent in the Pi SLFLs studied here (Figures 5 and 6). After initial study using various truncated forms of Pi SLF_2 to dissect its functional domains, we divided Pi SLF_2 into three domains, FD1, FD2, and FD3, with each containing one of three Pi SLF–specific regions (Figure 7A; see Supplemental Figure 6 and Supplemental Table 3 online), and examined the contributions of each domain to the interactions with S_3-RNase. Using various truncated forms of Pi SLF_2, with one or both FD domains deleted, we found that FD2 plays a major role in the strong interactions of Pi SLF_2 with S_3-RNase, a non-self S-RNase (Figure 7), whereas FD1 and FD3, each containing one of the two variable regions, appear to negatively modulate the interactions (Figure 7). The role of FD2 is further supported by the finding from the domain-swapping experiment that when it replaced the corresponding domain of Pi SLFLb-S_2, it conferred on the chimeric protein the ability to interact with S_3-RNase, although the interaction was not as strong as that between Pi SLF_2 and S_3-RNase (Figure 8).

Most importantly, the results of the domain-swapping experiment involving swapping FD1 alone, or both FD1 and FD3, between Pi SLF_1 and Pi SLF_2 (Figure 9) have revealed a functional role of these two domains in controlling the interactions between a Pi SLF and its self and non-self S-RNases. Specifically, we have shown that the interactions of Pi SLF_1 and Pi SLF_2 with S_2-RNase are completely reversed after their FD1 and FD3 have been swapped. That is, replacing FD1 and FD3 of Pi SLF_1 with the corresponding domains of Pi SLF_2 causes the chimeric protein to behave as Pi SLF_2 (the protein that contributes FD1 and FD3 to the chimeric protein), in that it interacts with S_2-RNase as weakly as does Pi SLF_2. Conversely, replacing FD1 and FD3 of Pi SLF_2 with the corresponding domains of Pi SLF_1 causes the chimeric protein to behave as Pi SLF_1 (the protein that contributes FD1 and FD3 to the chimeric protein), in that it interacts with S_2-RNase as strongly as does Pi SLF_1. Thus, FD1 and FD3 appear to be the prime candidates for the allelic specificity determinant of Pi SLF.

Based on the results of all of the domain-swapping experiments, we propose that Pi SLF has a conserved S-RNase binding domain (SBD) and a variable S-RNase binding regulating domain (SBRD). Many proteins contain both interacting and regulating domains for their binding to other proteins. For example, Bin1/M-amphiphysin-II contains two protein–protein interaction domains, the Src Homology3 (SH3) domain and the Exon 10 domain. The interaction between the SH3 domain and the Pro-rich domain of its interacting proteins is negatively regulated by the Exon 10 domain (Kojima et al., 2004). Our current model is that FD2 functions as an SBD and that FD1 and FD3 together function as an SBRD to regulate the interaction between SBD and S-RNases. One could envisage the following possibilities. In the case of non-self interactions, since there is no matching between FD1 and FD3 of a Pi SLF and its non-self S-RNases, the strong interactions between FD2 and a region common to all S-RNases would not be significantly affected. In the case of self interactions, the interactions between FD1 and FD3 of a Pi SLF and the matching allelic specificity determinant of its self S-RNase would cause conformational changes in the Pi SLF to weaken the otherwise strong interactions between FD2 and the self S-RNase.

In conclusion, the existence of Pi *SLFL* genes has allowed us to use comparative studies to investigate how Pi SLF interacts with S-RNase to mediate *S*-haplotype–specific inhibition of pollen tube growth, and the results have provided a biochemical explanation for our previous finding that a Pi SLF preferentially interacts with its non-self S-RNases (Hua and Kao, 2006). As the strong non-self interactions between Pi SLF and S-RNase appear to be critical for the function of Pi SLF in SI (possibly through mediating the degradation of non-self S-RNases in pollen tubes), our results have laid the foundation for future studies to fully understand the biochemical and molecular bases for the S-RNase–based SI mechanism.

METHODS

Plant Material

S_1S_1, S_1S_2, S_2S_2, S_2S_3, S_3S_3, and S_1S_3 genotypes of *Petunia inflata* were used in this study, and identification of these *S* genotypes was described by Ai et al. (1990).

cDNA Library Screening

The S_1 and S_2 pollen cDNA libraries used were constructed by Skirpan et al. (2001), and library screening was performed as described by Hua and Kao (2006), except for the use of Pi *SLF_2(CTD)* as a probe.

DNA and RNA Gel Blot Analyses

Genomic DNA was isolated from young leaves using Plant DNAzol reagent (Invitrogen) according to the manufacturer's protocol. Genomic DNA (10 to 15 μg) was digested overnight by various restriction enzymes as indicated. DNA gel blotting and hybridization were performed as described by Hua and Kao (2006), except that the temperatures for the low- and high-stringency hybridization conditions were 55 and 65°C, respectively. RNA gel blot analysis was performed as described by Hua and Kao (2006), and hybridization was performed under high-stringency conditions. The DNA probes used for both the genomic DNA gel blotting shown in Figure 1 and the RNA gel blotting shown in Figure 2 were obtained by PCR using a T3 primer (5′-ATTAACCCTCACTAAAGGGA-3′) and a T7 primer (5′-TAATACGACTCACTATAGGG-3′) to amplify the

corresponding cDNAs inserted in pBluescript SK− vector (Stratagene). The DNA probes used for the genomic DNA gel blotting shown in Supplemental Figure 2 online were obtained by PCR using specific primers (listed in Supplemental Table 4 online) to amplify cDNAs corresponding to the genes shown in Supplemental Figure 1 online.

RT-PCR Analysis

Total RNA was isolated from anthers at different developmental stages, mature pollen, pollen tubes, ovaries, styles, and leaves of an S_2S_2 plant as described by Hua and Kao (2006). Each RNA sample (5 μg) was used for cDNA synthesis in the presence (RT+) and absence (RT−) of Power Script reverse transcriptase according to the manufacturer's manual (Clontech). The RT+ products (0.2 μL each) were used for PCR to amplify the coding sequences of Pi *SLFLd-S*$_2$ and Pi *SLF*$_2$. The gene-specific primers used are shown in Supplemental Table 4 online. As controls, PCR was also performed for each RT+ and RT− product using primers specific to a gene encoding actin: 5′-GGCATCACACTTTCTACAATGAGC-3′ (forward) and 5′-GATATCCACATCACATTTCATGAT-3′ (reverse). All PCR procedures were performed as described by Wang et al. (2003) except for the following modifications: the annealing temperature for all three genes was 55°C; the times of extension were 90 s for Pi *SLFLd-S*$_2$ and Pi *SLF*$_2$ and 60 s for *Actin*, all at 72°C; the reactions were performed for 30 cycles for Pi *SLFLd-S*$_2$ and Pi *SLF*$_2$ and 20 cycles for *Actin*. The amplified products (20 μL each) were subjected to electrophoresis on 1% (w/v) agarose gels, and the gels were stained with ethidium bromide.

Generation of Ti Plasmid Constructs and Plant Transformation

The coding sequence for Pi *SLF*$_2$ was subcloned into pGEM-T Easy vector (Promega), and an *Nco*I restriction site was introduced at the 5′ end and a *Not*I site was introduced at the 3′ end by PCR. The 1.177-kb *Nco*I-*Not*I fragment containing the full-length Pi *SLF*$_2$ cDNA was released from pGEM-T Easy vector and used to replace the 0.72-kb *Nco*I-*Not*I fragment of the *GFP* coding sequence in *pLAT-GFP* (Dowd et al., 2006). The resulting construct, *pLAT52*-Pi *SLF*$_2$, contains Pi *SLF*$_2$ driven by the *LAT52* pollen-specific promoter of tomato (*Solanum lycopersicum*) (Twell et al., 1990). The *GFP* coding sequence was reamplified and a 39-nucleotide linker, encoding a 13–amino acid [$(Ala)_3(Gly)_{10}$] peptide linker, was inserted in front of the start codon of *GFP* by PCR using *pLAT-GFP* as template. A *Not*I restriction site was then introduced at both ends of the PCR product. The *Not*I fragment was inserted into the *pLAT52*-Pi *SLF*$_2$ to produce *pLAT52*-Pi *SLF*$_2$*:GFP*. The 2.553-kb *Sal*I-*Pst*I fragment, containing the *LAT52* promoter, Pi *SLF*$_2$, a 39-nucleotide linker, and the *GFP* coding sequence, was released from *pLAT52*-Pi *SLF*$_2$*:GFP* and inserted into the *Sal*I and *Pst*I sites of pBluescript SK− (Stratagene) to generate *pBluescript LAT52*-Pi *SLF*$_2$*:GFP*. A *Sac*I site was introduced at the 3′ end of the *LAT52*-Pi *SLF*$_2$*:GFP* insert. The *Sal*I/*Sac*I fragment was released from *pBluescript LAT52*-Pi *SLF*$_2$*:GFP* and used to replace the *Sal*I/*Sac*I fragment in *pBI101* (Clontech), which contains the GUS coding sequence, to yield *pBI LAT52*-Pi *SLF*$_2$*:GFP*. The *pBI LAT52*-Pi *SLFLc-S*$_1$*:GFP*, *pBI LAT52*-Pi *SLFLb-S*$_2$*:GFP*, and *pBI LAT52*-Pi *SLFLd-S*$_2$*:GFP* constructs were similarly generated using the coding sequences for Pi *SLFLc-S*$_1$, Pi *SLFLb-S*$_2$, and Pi *SLFLd-S*$_2$, respectively. The schemes for all of these constructs are shown in Supplemental Figure 1 online. All of the Ti plasmid constructs were separately electroporated into *Agrobacterium tumefaciens* strain LBA4404 (Invitrogen), and the *Agrobacterium*-mediated transformation was performed according to the procedure described previously (Lee et al., 1994).

Visualization of Pollen Tube Growth in Pollinated Pistils

Twenty hours after pollination, pollinated pistils (without ovaries) were fixed, macerated, and stained with 0.1% aniline blue dye according to the method described by Holden et al. (2003). Pollen tubes within different segments of the entire pistil (stigma plus style) were visualized with a Nikon Eclipse 90i epifluorescence microscope and recorded by a camera. All of the images of pollen tube growth within a pistil were integrated by Adobe Photoshop CS2.

Sequence Analysis

Amino acid sequences were aligned by ClustalW (http://www.ebi.ac.uk/clustalw/). A modified normed variability index method (Kheyr-Pour et al., 1990) was used to identify the Pi SLF–specific regions. For each alignment site, Pi SLF_1, Pi SLF_2, and Pi SLF_3 were used separately as a reference sequence for comparison with all of the other aligned sequences. If the amino acid residue of a sequence being compared with the reference sequence was the same as that of the reference sequence, an index number of −1 was assigned. If it was not, an index number of 1 was assigned. The total index value for each alignment site was calculated by summing all of the index numbers of the sequences compared. To better visualize regions that are specific to Pi SLF, a sliding window (a 60-alignment-site window with a 6-alignment-site slide) analysis of the total index value was performed and the value for each window was plotted against the first alignment site of that window. The variable regions among Pi SLF_1, Pi SLF_2, and Pi SLF_3 were determined by the normed variability index analysis as described by Kheyr-Pour et al. (1990). To identify the regions of Pi *SLF* that are under positive selection, Ka/Ks values were calculated for pairwise comparisons among Pi *SLF*$_1$, Pi *SLF*$_2$, and Pi *SLF*$_3$ using the K-estimator 6.1 software package (Comeron, 1999) with a 180-nucleotide window and an 18-nucleotide slide.

Expression and Purification of Recombinant Proteins

The DNA fragments containing coding sequences for all of the full-length and truncated genes described in the text and listed in Supplemental Table 3 online were obtained by PCR using the primers listed in Supplemental Table 4 online, and the fragments were subcloned separately in-frame behind the sequence for the $(His)_6$:T7 tag in vector pET28 (Novagen) or in-frame behind the GST coding sequence in vector pGEX-5X-1 (GE Healthcare). The DNA fragments containing coding sequences for the chimeric fusion proteins shown in Figures 8 and 9 were obtained by overlap PCR using the primers listed in Supplemental Table 4 online, and the fragments were subcloned separately into pET28 (Novagen) in-frame behind the $(His)_6$:T7 tag. All of the recombinant proteins were expressed at 18°C in BL21 Codon Plus *Escherichia coli* (Stratagene) and purified using HIS-Select HF Nickel Affinity Gel (Sigma-Aldrich) or Glutathione Sepharose 4 Fast Flow affinity beads (GE Healthcare), according to each manufacturer's procedure.

In Vitro Protein Binding and Competition Assays

The in vitro protein binding assay was performed using GST:S_3-RNase attached to Glutathione Sepharose 4 Fast Flow affinity beads and $(His)_6$:T7-tagged proteins, as described previously (Hua and Kao, 2006), except for the use of a modified binding buffer (50 mM Tris-HCl, pH 7.5, 5 mM $MgCl_2$, 150 mM NaCl, 2 mM DTT, 0.01% Nonidet P-40, and 5% glycerol). All of the $(His)_6$:T7-tagged proteins were first tested to ensure that they did not interact with GST under the same binding assay conditions. The competition assay was performed similarly except for the following modifications. The amount of GST:S_3-RNase bound to the Glutathione Sepharose beads was decreased to one-twentieth of the amount used for the protein binding assay, and equal amounts of $(His)_6$:T7-tagged proteins, $(His)_6$:T7:Pi SLF_2 and $(His)_6$:T7:Pi SLFLb-S_2, were used in the same binding reaction. After a 90-min incubation in the

competition binding buffer (50 mM Tris-HCl, pH 7.5, 5 mM $MgCl_2$, 250 mM NaCl, 2 mM DTT, 0.01% Nonidet P-40, and 5% glycerol) at room temperature with gentle rotating, the beads were thoroughly washed four to five times with binding buffer. The bound proteins were eluted and analyzed by immunoblotting as was done in the protein binding assay.

Immunoblot Analysis

Immunoblot analysis of the $(His)_6$:T7-tagged proteins was performed as described previously (Hua and Kao, 2006). Total pollen tube extracts used in Figure 3A were prepared as described previously (Hua and Kao, 2006), and the total proteins of stage 5 anthers used in Figure 3B were extracted with the same extraction buffer described by Lee et al. (1994), except that both extract buffers contained 1% protease inhibitor cocktail (Sigma-Aldrich). GFP and its fusion proteins were detected by a rabbit anti-GFP antibody (Abcam).

Accession Numbers

The new sequence data identified in this article can be found in the GenBank data library under the following accession numbers: Pi *SLFLa-S1* (EF614190), Pi *SLFLa-S2* (EF614189), Pi *SLFLb-S2* (EF614188), Pi *SLFLc-S1* (EF614191), Pi *SLFLd-S2* (EF614187). The accession numbers for the previously identified sequence data used in this article are as follows: Pi SLF_1 (AAS79484), Pi SLF_2 (AAS79485), Pi SLF_3 (AAS79486), $S_1(S_2)$-A113 (AAR15911), S_1-A134 (AAR15914), S_2-A134 (AAR15915), S_3-A134 (AAR15916) from *Petunia inflata*; Ah SLF_2 (CAC33010) from *Antirrhinum hispanicum*.

Supplemental Data

The following materials are available in the online version of this article.

Supplemental Figure 1. Schemes of the Ti Plasmid Constructs Used in Plant Transformation Experiments.

Supplemental Figure 2. Genomic DNA Gel Blots Showing Independent Transgenic Lines That Contain a Single Insert of Pi *SLF2:GFP*, Pi *SLFLb-S2:GFP*, Pi *SLFLc-S1:GFP*, or Pi *SLFLd-S2:GFP*.

Supplemental Figure 3. Bright-Field (Top) and Fluorescence (Bottom) Images of Representative Pollen Tubes Produced by a Progeny Plant from a Cross between a Wild-Type S_2S_3 Plant and the Transgenic Plant S_2S_3/Pi *SLF2:GFP*-5.

Supplemental Figure 4. Fluorescence Images of Pollen Tubes in Pistils of a Wild-Type S_2S_3 Plant at 20 h after Pollination with Pollen from Transgenic Plant S_2S_3/Pi *SLFLd-S2:GFP*-30, Another Wild-Type S_2S_3 Plant, Transgenic Plant S_2S_3/Pi *SLF2:GFP*-5, and a Wild-Type S_1S_1 Plant.

Supplemental Figure 5. Ponceau S Staining of the Immunoblots Containing Binding Assays Conducted at High Concentrations to Show That the Amount of GST:S_3-RNase Used in Each Binding Reaction was in Large Excess over the $(His)_6$:T7-Tagged Protein.

Supplemental Figure 6. Alignment of the Deduced Amino Acid Sequences of Three Allelic Variants of Pi SLF.

Supplemental Table 1. Percentage Pairwise Nucleotide Sequence Identities between the Coding Regions of Pi *SLF* and Pi *SLFL* Genes.

Supplemental Table 2. Percentage Pairwise Sequence Identities between Deduced Amino Acid Sequences of Pi *SLF* and Pi *SLFL* Genes.

Supplemental Table 3. List of Recombinant Proteins Involved in This Study.

Supplemental Table 4. List of PCR Primers Used in This Study.

ACKNOWLEDGMENTS

We thank Yan Wang for technical help in the initial phase of this work and Peter Dowd for providing the *pLAT-GFP* construct and for technical advice. We also thank Peter Dowd, Allison Fields, and Ning Wang for valuable comments on the manuscript, Anthony Omeis for greenhouse management, and Jiong Wang for general laboratory help. This work was supported by Grant IOB-0543201 from the National Science Foundation to T.-h.K.

Received September 5, 2007; revised October 19, 2007; accepted October 24, 2007; published November 16, 2007.

REFERENCES

Ai, Y., Singh, A., Coleman, C.E., Ioerger, T.R., Kheyr-Pour, A., and Kao, T.-h. (1990). Self-incompatibility in *Petunia inflata*: Isolation and characterization of cDNAs encoding three *S*-allele-associated proteins. Sex. Plant Reprod. **3:** 130–138.

Cardozo, T., and Pagano, M. (2004). The SCF ubiquitin ligase: Insights into a molecular machine. Nat. Rev. Mol. Cell Biol. **5:** 739–751.

Comeron, J.M. (1999). K-Estimator: Calculation of the number of nucleotide substitutions per site and the confidence intervals. Bioinformatics **15:** 763–764.

de Nettancourt, D. (2001). Incompatibility and Incongruity in Wild and Cultivated Plants. (Berlin: Springer-Verlag).

Dowd, P.E., Coursol, S., Skirpan, A., Kao, T.-h., and Gilroy, S. (2006). *Petunia* phospholipase C1 is involved in pollen tube growth. Plant Cell **18:** 1438–1453.

Entani, T., Zwano, M., Shiba, H., Che, F.S., Isogai, A., and Takayama, S. (2003). Comparative analysis of the self-incompatibility (*S*-) locus region of *Prunus mume*: Identification of a pollen-expressed F-box gene with allelic diversity. Genes Cells **8:** 203–213.

Gagne, J.M., Downes, B.P., Shiu, S.H., Durski, A.M., and Vierstra, R.D. (2002). The F-box subunit of the SCF E3 complex is encoded by a diverse superfamily of genes in Arabidopsis. Proc. Natl. Acad. Sci. USA **99:** 11519–11524.

Goldraij, A., Kondo, K., Lee, C.B., Hancock, C.N., Sivaguru, M., Vazquez-Santana, S., Kim, S., Phillips, T.E., Cruz-Garcia, F., and McClure, B. (2006). Compartmentalization of S-RNase and HT-B degradation in self-incompatible *Nicotiana.* Nature **439:** 805–810.

Holden, M.J., Marty, J.A., and Singh-Cundy, A. (2003). Pollination-induced ethylene promotes the early phase of pollen tube growth in *Petunia inflata.* J. Plant Physiol. **160:** 261–269.

Hua, Z.H., and Kao, T.-h. (2006). Identification and characterization of components of a putative *Petunia S*-locus F-box-containing E3 ligase complex involved in S-RNase–based self-incompatibility. Plant Cell **18:** 2531–2553.

Huang, S., Lee, H.-S., Karunanandaa, B., and Kao, T.-h. (1994). Ribonuclease activity of *Petunia inflata* S proteins is essential for rejection of self-pollen. Plant Cell **6:** 1021–1028.

Kao, T.-h., and Tsukamoto, T. (2004). The molecular and genetic bases of S-RNase-based self-incompatibility. Plant Cell **16** (suppl.): S72–S83.

Kheyr-Pour, A., Bintrim, S.C., Ioerger, T.R., Remy, R., Hammond, S.A., and Kao, T.-h. (1990). Sequence diversity of pistil S-proteins associated with gametophytic self-incompatibility in *Nicotiana alata.* Sex. Plant Reprod. **3:** 88–97.

Kojima, C., Hashimoto, A., Yabuta, I., Hirose, M., Hashimoto, S., Kanaho, Y., Sumimoto, H., Ikegami, T., and Sabe, H. (2004). Regulation of Bin1 SH3 domain binding by phosphoinositides. EMBO J. **23:** 4413–4422.

Lai, Z., Ma, W., Han, B., Liang, L., Zhang, Y., Hong, G., and Xue, Y. (2002). An F-box gene linked to the self-incompatibility (*S*) locus of *Antirrhinum* is expressed specifically in pollen and tapetum. Plant Mol. Biol. **50:** 29–42.

Lee, H.-S., Huang, S., and Kao, T.-h. (1994). S proteins control rejection of incompatible pollen in *Petunia inflata.* Nature **367:** 560–563.

Lee, H.-S., Karunanandaa, B., McCubbin, A., Gilroy, S., and Kao, T.-h. (1996). PRK1, a receptor-like kinase of *Petunia inflata*, is essential for postmeiotic development of pollen. Plant J. **9:** 613–624.

Luu, D.-T., Qin, K., Laublin, G., Yang, Q., Morse, D., and Cappadocia, M. (2001). Rejection of *S*-heteroallelic pollen by a dual-specific S-RNase in *Solanum chacoense* predicts a multimeric SI pollen component. Genetics **159:** 329–335.

Luu, D.-T., Qin, X., Morse, D., and Cappadocia, M. (2000). S-RNase uptake by compatible pollen tubes in gametophytic self-incompatibility. Nature **407:** 649–651.

McClure, B.A., Gray, J.E., Anderson, M.A., and Clarke, A.E. (1990). Self-incompatibility in *Nicotiana alata* involves degradation of pollen rRNA. Nature **347:** 757–760.

McCubbin, A.G., Wang, X., and Kao, T.-h. (2000). Identification of selfincompatibility (*S*-) locus linked pollen cDNA markers in *Petunia inflata.* Genome **43:** 619–627.

Moon, J., Parry, G., and Estelle, M. (2004). The ubiquitin-proteasome pathway and plant development. Plant Cell **16:** 3181–3195.

Murfett, J., Atherton, T.L., Mou, B., Gasser, C.S., and McClure, B.A. (1994). S-RNase expressed in transgenic *Nicotiana* causes *S*-allele-specific pollen rejection. Nature **367:** 563–566.

Qiao, H., Wang, F., Zhao, L., Zhou, J., Lai, Z., Zhang, Y., Robbins, T.P., and Xue, Y. (2004a). The F-box protein Ah SLF-S_2 controls the pollen function of S-RNase-based self-incompatibility. Plant Cell **16:** 2307–2322.

Qiao, H., Wang, H., Zhao, L., Zhou, J., Huang, J., Zhang, Y., and Xue, Y. (2004b). The F-box protein Ah SLF-S_2 physically interacts with S-RNases that may be inhibited by the ubiquitin/26S proteasome pathway of protein degradation during compatible pollination in *Antirrhinum.* Plant Cell **16:** 582–595.

Risseeuw, E.P., Daskalchuk, T.E., Banks, T.W., Liu, E., Cotelesage, J., Hellmann, H., Estelle, M., Somers, D.E., and Crosby, W.L. (2003). Protein interaction analysis of SCF ubiquitin E3 ligase subunits from *Arabidopsis.* Plant J. **34:** 753–767.

Sassa, H., Kakui, H., Miyamoto, M., Suzuki, Y., Hanada, T., Ushijima, K., Kusaba, M., Hirano, H., and Koba, T. (2007). *S* locus *F-box brothers*: Multiple and pollen-specific F-box genes with *S* haplotype-specific polymorphisms in apple and Japanese pear. Genetics **175:** 1869–1881.

Sijacic, P., Wang, X., Skirpan, A.L., Wang, Y., Dowd, P.E., McCubbin, A.G., Huang, S., and Kao, T.-h. (2004). Identification of the pollen determinant of S-RNase-mediated self-incompatibility. Nature **429:** 302–305.

Sims, T.L., and Ordanic, M. (2001). Identification of a S-ribonuclease binding protein in *Petunia hybrida.* Plant Mol. Biol. **47:** 771–783.

Skirpan, A.L., McCubbin, A.G., Ishimizu, T., Wang, X., Hu, Y., Dowd, P.E., Ma, H., and Kao, T.-h. (2001). Isolation and characterization of kinase interacting protein 1, a pollen protein that interacts with the kinase domain of PRK1, a receptor-like kinase of petunia. Plant Physiol. **126:** 1480–1492.

Smalle, J., and Vierstra, R.D. (2004). The ubiquitin 26S proteasome proteolytic pathway. Annu. Rev. Plant Biol. **55:** 555–590.

Sonneveld, T., Kenneth, R., Tobutt, K.R., Simon, P., Vaughan, S.P., and Robbins, T.P. (2005). Loss of pollen-*S* function in two self-compatible selections of *Prunus avium* is associated with deletion/mutation of an *S* haplotype-specific F-box gene. Plant Cell **17:** 37–51.

Tsukamoto, T., Hauck, N.R., Tao, R., Jiang, N., and Iezzoni, A.F. (2006). Molecular characterization of three non-functional *S*-haplotypes in sour cherry (*Prunus cerasus*). Plant Mol. Biol. **62:** 371–383.

Twell, D., Yamaguchi, J., and McCormick, S. (1990). Pollen-specific gene expression in transgenic plants: Coordinate regulation of two different tomato gene promoters during microsporogenesis. Development **109:** 705–713.

Ushijima, K., Sassa, H., Dandekar, A.M., Gradziel, T.M., Tao, R., and Hirano, H. (2003). Structural and transcriptional analysis of the self-incompatibility locus of almond: Identification of a pollen-expressed F-box gene with haplotype-specific polymorphism. Plant Cell **15:** 771–781.

Xue, Y., Carpenter, R., Dickinson, H.G., and Coen, E.S. (1996). Origin of allelic diversity in *Antirrhinum S* locus RNases. Plant Cell **8:** 805–814.

Wang, Y., Tsukamoto, T., Yi, K.-w., Wang, X., Huang, S., McCubbin, A.G., and Kao, T.-h. (2004). Chromosome walking in the *Petunia inflata* self-incompatibility (*S*-) locus and gene identification in an 881-kb contig containing *S_2-RNase.* Plant Mol. Biol. **54:** 727–742.

Wang, Y., Wang, X., McCubbin, A.G., and Kao, T.-h. (2003). Genetic mapping and molecular characterization of the self-incompatibility (*S*) locus in *Petunia inflata.* Plant Mol. Biol. **53:** 565–580.

Zhou, J., Wang, F., Ma, W., Zhang, Y., Han, B., and Xue, Y. (2003). Structural and transcriptional analysis of *S*-locus F-box (*SLF*) genes in *Antirrhinum.* Sex. Plant Reprod. **16:** 165–177.